



## Article

# Meat-Processing Wastewater Treatment Using an Anaerobic Membrane Bioreactor (AnMBR)

Ferdinand Hummel <sup>1,\*</sup> , Lisa Bauer <sup>2</sup> , Wolfgang Gabauer <sup>1</sup> and Werner Fuchs <sup>1,\*</sup> <sup>1</sup> IFA-Tulln, BOKU University, 3430 Tulln an der Donau, Austria; wolfgang.gabauer@boku.ac.at<sup>2</sup> BEST-Bioenergy and Sustainable Technologies GmbH, Inffeldgasse 21b, 8010 Graz, Austria; lisa.bauer@best-research.eu

\* Correspondence: ferdinand.hummel@boku.ac.at (F.H.); werner.fuchs@boku.ac.at (W.F.); Tel.: +43-6506621237 (F.H.); +43-14765497401 (W.F.)

**Abstract:** This study explores AnMBR technology as a promising method for treating wastewater from the meat-processing industry by analysing its characteristics and impact under continuous feeding. The solids were retained, utilising an ultrafiltration membrane with a pore size of 0.2 µm, and the efficacy of reducing the organic load was evaluated. Although the COD removal rate decreased from 100% at an OLR of 0.71 g/(L\*d) to 73% at an OLR of 2.2 g/(L\*d), maximum methane yields were achieved at the highest OLR, 292.9 Nm<sup>3</sup>/t (COD) and 397.8 Nm<sup>3</sup>/t (VS) per loaded organics and 353.1 Nm<sup>3</sup>/t (COD) and 518.7 Nm<sup>3</sup>/t (VS) per removed organics. An analysis of the microbial community was performed at the end of the experiment to assess the effects of the process and the substrate on its composition. The AnMBR system effectively converts meat-processing wastewater into biogas, maintaining high yields and reducing the loss of dissolved methane in the permeate, thanks to a temperature of 37 °C and high salt levels. AnMBR enables rapid start-up, efficient COD removal, and high biogas yields, making it suitable for treating industrial wastewater with high organic loads, enhancing biogas production, and reducing methane loss. Challenges such as high salt and phosphate levels present opportunities for a wider use in nutrient recovery and water reclamation.

**Keywords:** anaerobic digestion; water recovery; dissolved methane; COD removal; food-processing industry; microbial community analysis; biomethane production; ceramic membrane; MBR; membrane bioreactor; hydrogenotrophic archaea; methanobacteria



Academic Editor: Giulia Bozzano

Received: 30 December 2024

Revised: 26 January 2025

Accepted: 28 January 2025

Published: 1 February 2025

**Citation:** Hummel, F.; Bauer, L.; Gabauer, W.; Fuchs, W. Meat-Processing Wastewater Treatment Using an Anaerobic Membrane Bioreactor (AnMBR). *Fermentation* **2025**, *11*, 68. <https://doi.org/10.3390/fermentation11020068>

**Copyright:** © 2025 by the authors. Licensee MDPI, Basel, Switzerland. This article is an open access article distributed under the terms and conditions of the Creative Commons Attribution (CC BY) license (<https://creativecommons.org/licenses/by/4.0/>).

## 1. Introduction

In light of the increasing energy demands driven by population growth [1] and the ongoing natural gas crisis in Europe [2], there is an urgent need for alternative energy sources. Therefore, the EU Commission launched the European Green Deal, aiming at a reduction in net greenhouse gas emissions by at least 55% by 2030 compared to 1990 levels. To achieve these targets, the Austrian government has established ambitious goals to achieve 100% renewable electricity by 2030 and operate with net zero CO<sub>2</sub> emissions by 2040 [3]. This requires a significant reduction in the dependence on natural gas, which can be partially substituted with biogenic methane derived from various organic waste materials. To facilitate this transition, it is essential to explore all available biogenic residues for anaerobic digestion.

In particular, in light of the “food versus fuel” debate, the focus has changed toward the usage of residues and waste for biogas production. Consequently, wastewater and wastewater treatment plants have emerged as critical sources of material and energy

recovery, offering the dual benefit of resource recovery and waste management. The anaerobic digestion of wastewater presents several advantages over traditional aerobic wastewater treatment methods, including lower energy requirements, reduced sludge volumes and the potential for net energy production from biogenic contaminants [1–3].

Despite advances in wastewater treatment technologies using anaerobic digestion, the high volume and dilution of biogenic materials in wastewater pose significant challenges, such as the low growth rate of anaerobic microorganisms [4]. A balanced microbial composition of the sludge inside the reactor is essential for biogas production. Therefore, preventing the washout of methanogenic archaea, which are critical for converting intermediates to methane, is essential because of their low growth rate. High hydraulic retention times (HRTs) are required in classical biogas systems to give the microorganisms enough time to convert organic matter to biogas [4], preventing the usage of wastewater as substrate.

To address this issue, various biogas reactor designs have been developed. The most prominent example is the Upflow Anaerobic Sludge Blanket reactor (UASB). Reactors of this type are particularly effective in treating high-strength wastewater without losing methanogenic microorganisms. Nevertheless, this system has not been proven suitable for low-strength wastewater [5]. Furthermore, the recovery of fresh water from wastewater is increasingly critical due to the increased risks of droughts intensified by climate change and unsustainable water use practices. Recent studies by Rodell et al. highlight the alarming decline in freshwater resources, emphasising the need for innovative treatment solutions [6].

A promising technology that addresses both of the above-mentioned challenges is the AnMBR, which integrates membrane filtration with anaerobic digestion. This system not only prevents the washout of methanogens, but also produces a particle-free permeate that can be further treated for reuse [1,2]. However, challenges such as membrane fouling, high energy consumption, and loss of dissolved methane remain significant barriers to widespread adoption [3,7,8]. There are various AnMBR configurations with different advantages [9], but the set-up with an external cross-flow membrane is the most robust since fouling can be prohibited by applying cross-flow velocities of 2–3 m/s [10]. Higher cross-flow velocities could adversely affect biomass activities due to increased shear forces [2].

Currently, AnMBRs are more competitive in treating high-strength wastewater, such as that generated by the food and beverage industry, where energy and cost savings can be substantial [11]. A main advantage is also the reduced amount of anaerobic sludge that has to be deployed to fields, disposed of in landfills, or, in the future, burnt due to EU regulation, which would further increase costs and effort for conventional wastewater treatment plants.

The meat-processing industry, which generates large volumes of high-strength wastewater, is expected to benefit from these advances. While there have been improvements in wastewater treatment in this sector, the high demands of energy and water in the industry require further innovations [11–14]. Although there are low-tech treatment options for red meat processors, such as anaerobic lagoons, these are not applicable to a country such as Austria with limited space and low average temperatures. Moreover, the wastewater of meat-processing facilities contains high amounts of fat, which would float up and not settle in lagoons. Therefore, high-tech solutions are required for treatment and can additionally be combined with water recovery, which would also be required for reuse in a lagoon setting. One such high-tech solution could be membrane bioreactors. The potential for energy and cost reductions using membrane bioreactors in this context could reach 49% [15].

Due to its advantages, there have already been several studies on the treatment of slaughterhouse wastewater using AnMBR technology [16–18], but slaughterhouse opera-

tions are often separated from other meat-processing operations, and therefore, there are cases where meat-processing and slaughterhouse wastewater are treated separately. The wastewater of meat-processing operations differs in their composition, as less blood and protein are contained, but more fat is contained from cooking procedures, and applied additives and salts are contained in the wastewater [19].

To fill this knowledge gap, this study aimed to elaborate the potential application of AnMBR technology in the meat-processing industry by investigating the characteristics of wastewater from a meat-processing operation and the implications of anaerobic digestion experiments in an AnMBR system with continuous feeding.

## 2. Materials and Methods

### 2.1. Substrate

The industrial wastewater used as a substrate in the experiments originated from a meat-processing operation located in Lower Austria. The factory is one of the largest meat product suppliers in Austria. The production facilities generate a wastewater flow of up to 650 m<sup>3</sup> per day, which represents the major contribution in volume, as well as chemical oxygen demand (COD), nitrogen, and phosphorous load, to the local municipal wastewater treatment plant.

The wastewater was collected directly from the sewer with a submersible pump, pumped into 60 l barrels, and stored at 4 °C until usage. Each wastewater barrel was sampled and analysed for its volatile fatty acid (VFA) content, total solids (TS) and volatile solids (VS), COD, total Kjeldahl nitrogen (TKN), and ammonium nitrogen (NH<sub>4</sub>-N) content. In addition, the biomethane potential (BMP) was analysed using two distinct inocula. The methods for all of these parameters are described in Section 2.3.

### 2.2. Experimental Set-Up

#### 2.2.1. Set-Up of the Lab-Scale AnMBR

Images as well as a scheme of the set-up of the lab-scale AnMBR are shown in Figure 1. It was composed of an (I) external ceramic ultrafiltration unit (UF) (pore size: 0.2 µm, area: 0.117 m<sup>2</sup>) coupled to a (II) recirculation pump (NIROSTAR 2000-C/PF, ZUWA-Pumpe GmbH, Laufen, Germany) and a continuously stirred tank reactor (CSTR) with a total volume of 11 L and a head space of 2 L. The total working volume including the periphery of the reactor (hoses and pump volume) was 18.6 l of anaerobic sludge. Crossflow velocity was set to 2.5 m/s by a frequency converter. Permeate release was controlled with an (III) automated valve. The weight of the feed and the permeate were recorded by two (IV) balances (CDS 60K0.2, KERN & Sohn GmbH, Balingen, Germany). The feed was applied with a (V) peristaltic pump (505U, Watson-Marlow Limited, Falmouth, UK). The reactor tank was equipped with a (VI) heating jacket, a temperature indicator, and controller keeping the temperature constant at 37 °C. A (VII) stirrer was attached from the top, constantly stirring at 25 rpm to avoid dead spots. The produced biomethane of the AnMBR was collected after a (VIII) Ritter Gas clock (TG0.5/5, Dr.-Ing. RITTER Apparatebau GmbH & Co. KG, Bochum, Germany) in a 5 L gasbag (30228-U, SUPELCO, Bellefonte, PA 16823, USA). Once the gas clock registered 3.5 L biogas, the gas bag was automatically sampled and measured with an automated gas analyser (AwiFlex Cool+, Awite Bioenergie GmbH, LangenbaFch, Germany) for its CH<sub>4</sub>, CO<sub>2</sub>, O<sub>2</sub>, H<sub>2</sub>, and H<sub>2</sub>S composition. The measurement range for CH<sub>4</sub> and CO<sub>2</sub> is between 0 and 100% with a reproducibility of ±0.1%, and the O<sub>2</sub> range is between 0 and 25% ± 0.25%; for H<sub>2</sub>, the range is from 0 to 50,000 ppm ± 0.1% and from 0 to 10,000 ppm for H<sub>2</sub>S, with a reproducibility of ±2.5% for up to 20 ppm, ±1.3% for up to 500 ppm, and ±1.0% for up to 10,000 ppm.

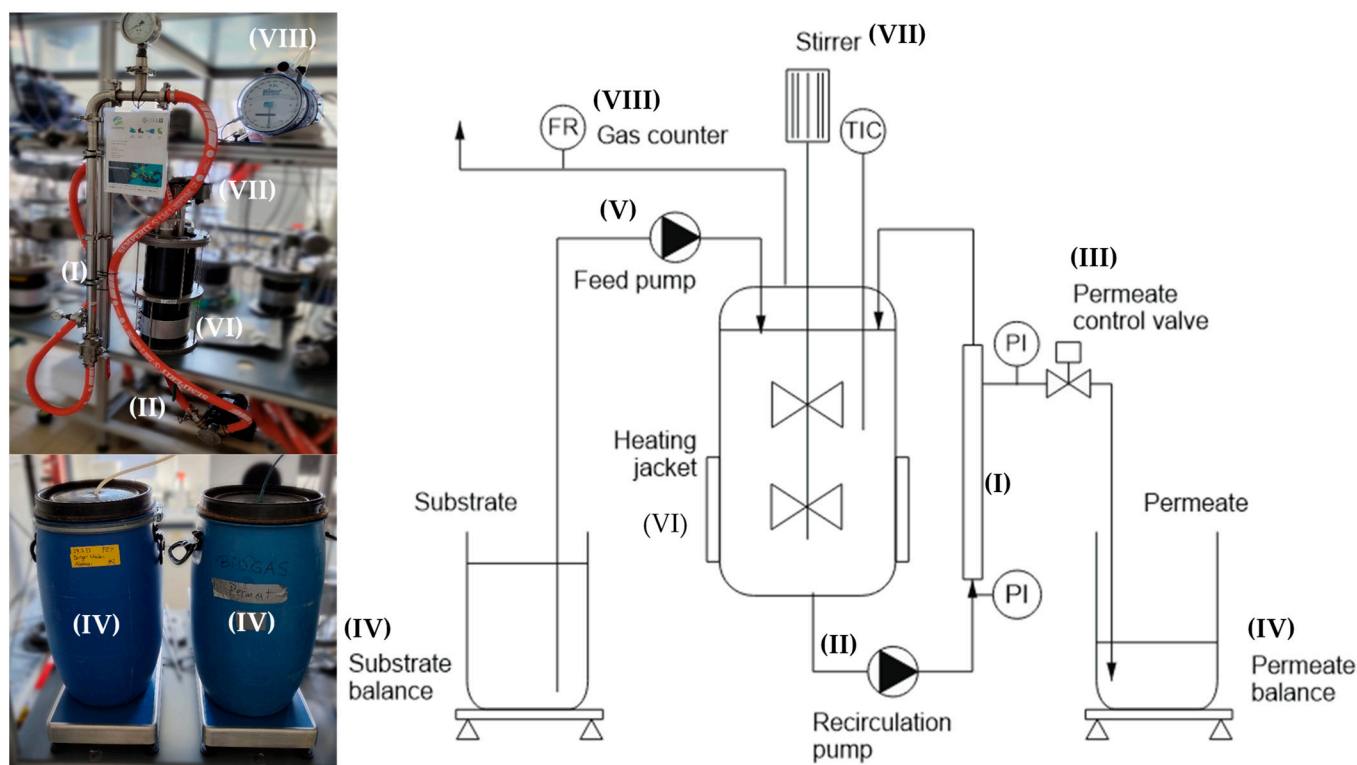


**Figure 1.** Experimental setup of the AnMBR used in the continuous experiment; composed of an (I) external ceramic ultrafiltration unit, (II) recirculation pump and a stirred tank reactor, (III) automated valve for permeate release, (IV) balance for feed and permeate, (V) peristaltic pump for feed application, (VI) heating jacket and TIC for constant reactor temperature (37 °C), (VII) stirrer (25 rpm) to avoid dead spots, and (VIII) Ritter Gas clock.

For the continuous feeding experiment, the feeding rate was set in g/h in the in-house software controlling the permeate release. The permeate valve opened according to the feeding plan until the calculated amount was registered by the balance. Subsequently, fresh substrate was supplied to the reactor by the feed pump, which was switched off once the software registered the withdrawal of an equivalent amount on the feed balance. Through this control algorithm, the reactor level was kept constant.

### 2.2.2. Continuous Feeding Experiment

For AnMBR inoculation, fresh anaerobic sludge was obtained from the nearby municipal wastewater treatment plant (WWTP) in Tulln, AT. The feeding of wastewater commenced only after biogas production of the original sludge had ceased. The feeding experiment was initiated after a two-week adaptation period, minimising the risk of shock loading.

The feeding rate was systematically increased from an initial rate of 50 g/h to a maximum of 750 g/h over a total duration of 11 weeks. The wastewater was pumped directly into the reactor from 60 L storage barrels. To maintain homogeneity and prevent settlement of solids, a small garden fountain pump was submerged in the barrel. This ensured an even distribution and consistent supply with the different constituents of the wastewater. The initial substrate weight in each barrel was approximately 37–40 kg, and they were replaced once they reached a residual weight of 5 kg.

Throughout the experiment, the feed barrel, permeate stream, and reactor content were sampled weekly. Samples were analysed for their VFA, TS, VS, COD, TKN, and  $\text{NH}_4\text{-N}$  content. At the end of the experiment, a comprehensive analysis of the anaerobic microbial community was conducted.

### 2.3. Analytical Methods

#### 2.3.1. Biomethane Potential (BMP) Tests and Inhibition Tests

BMP tests were carried out in triplicate according to the VDI 4630 (2006) guidelines as described by Ortner et al. 2014 [20] with two different inocula. The standard inoculum was composed of a mixture of anaerobic sludge sourced from a biogas plant and sludge from a wastewater treatment plant in a 1:1 ratio on a wet mass basis, resulting in a TS of 3.50% and a VS of 2.98% per fresh matter (FM). The second inoculum used was freshly sourced from the lab AnMBR with a TS of 1.32% and a VS of 0.75% per FM. The AnMBR was originally filled with anaerobic sludge from a wastewater treatment plant. Batch tests were conducted in triplicate, and blanks with no added substrate were also run in triplicate. At the beginning of the continuous feeding experiment, a BMP test with each inoculum was performed with a VS substrate-to-inoculum ratio (SIR) of 0.4. Another batch test was conducted on day 29 of the continuous feeding experiment with freshly sampled AnMBR inoculum and wastewater. The first batch tests were subsequently used for a fed-batch experiment using sucrose as a second substrate to test for inhibitions of the wastewater on the microbial degradation process. The sucrose was used as an easily available substrate, and therefore, a lower VS SIR of 0.18 was used. For further details, see Appendix A.

#### 2.3.2. Chemical Parameters

Before sample preparation was started, the samples stored at 4 °C were brought to room temperature. The wastewater used for chemical analysis was additionally mixed with an ULTRA-TURRAX T50 at 6000 rpm (Janke&Kunkel IKA-Labortechnik, 79219 Staufen, Germany) for homogenisation and to emulsify the fat. The chemical parameters were measured using standard methods. The TS, VS, and the COD of the wastewater, feed, reactor content, and the permeate were analysed according to the methods described in DIN DEV 38 414 [21] part 2, DIN DEV 38 414 [21] part 3, and DIN DEV 38409-H41-1 [22], respectively. The samples for the TKN analysis were digested with sulphuric acid, followed by distillation and subsequent titration of ammonia (DIN 19 684, part 4 [23]). To estimate the protein content, the TKN was converted using the traditional fixed conversion factor of 6.25 not related to any specific feedstock, assuming that 1 kg of plant or animal protein contains 160 g N [24]. NH<sub>4</sub>-N was analysed with the same method without the digestion step. VFAs were determined according to the standard method DIN 38 414-19 [25] by HPLC, preceded by a Carrez precipitation step. A detailed description of all analytical procedures, as well as the set-up and operation conditions of laboratory investigations, is given by Ortner et al. [7]. The total phosphate (PO<sub>4</sub>-P) contents in the permeate and the feed were determined with an LCK350 Hach Lange cuvettes test (Hach Lange GmbH, Düsseldorf, Germany) according to the manufacturer's instructions.

#### 2.3.3. Fat Content

The extraction of raw fats was conducted in a Soxtherm apparatus (Soxtherm 2000, Variostat, C. Gerhardt GmbH & Co. KG, Königswinter, Germany) using lyophilised wastewater samples. A solvent mixture of 60% chloroform and 40% methanol was used. The protocol included an initial 1 h cooking phase, followed by an extraction stage at 260 °C for 1 h and 20 min, during which 15 mL of solvent was automatically added in four increments. The extraction procedure utilised approximately 0.3–0.5 g of the freeze-dried sample. Post-extraction, the solvent was evaporated at ambient temperature, and the residual extract was weighed using an analytical scale (Adventurer, AR3130, OHAUS Corp., Parsippany, NJ 07054, USA). The extract was subsequently re-dissolved in 20 mL of chloroform and filtered through glass filters (Por 1, P160, 100–160 µm, ROBU-GLAS Filter, 57644 Hattert,



Germany) to segregate fats from methanol-dissolved salts. The solvent was evaporated at 60 °C, and the weight of extracted fats was determined using the analytical scale.

#### 2.3.4. Theoretical Methane Yield from Substrate Composition

The VS composition was estimated based on the fat content and protein calculated from the TKN. The remaining unexplained VS was assumed to be carbohydrates. From this composition, the theoretical yield was calculated based on Baserga and Rutzmoser [26,27].

#### 2.3.5. Anions

Anions were quantified using an ICS-900 system from Dionex Thermo Scientific (Waltham, MA 02451, USA), equipped with an AS-DV autosampler and a conductivity detector. The system was operated using an AG14A (4 × 50 mm) guard column and an AS14A (4 × 250 mm) analytical column (Thermo Fisher Scientific Inc., Waltham, MA 02451, USA). An 8 mM Na<sub>2</sub>CO<sub>3</sub> and 1 mM NaHCO<sub>3</sub> solution was used as eluent at an isocratic flow rate of 1 mL/min. The suppressor (ACRS 500) was regenerated with a 57 mM H<sub>2</sub>SO<sub>4</sub> solution at an equivalent flow rate. All solutions were prepared using ultrapure water obtained from an Arium system (Sartorius, 37079 Göttingen, Germany). Calibration was carried out using a mixed standard of all target anions (chloride, nitrate, phosphate, and sulphate) within a concentration range of 1 mg/L up to 500 mg/L. Calibration standards were injected in triplicate, and the determination limit and detection limit were calculated following DIN 32645, operating within the linear calibration range of the conductivity detector. The performance of the system was monitored using standards at the beginning of each sequence and after every 10 samples.

#### 2.3.6. Dissolved Methane

For the measurement of methane, 3 × 60 mL of the permeate were filled into 100 mL serum flasks and sealed with gas-tight stoppers. After equilibration on a shaker at room temperature for 1 h, the gas phase in the flasks was sampled with a gas-tight 250 µL Hamilton syringe and injected into a gas chromatograph (7890A-G3440A, column 19095P-Q04, Agilent Technologies, Santa Clara, CA, USA) equipped with a flame ionisation detector (280 °C), with H<sub>2</sub> as carrier gas (flow of 30 mL/min). The temperature and pressure programmes were as follows: 7.8 min at 30 °C, 35 kPa, then 2 min +60 °C/min, +5 kPa/min, then 8 min at 150 °C, +5 kPa/min to 45 kPa. The system was calibrated in a range of 1.01–87.42% methane with a deviation of ±0.16% in the used measurement range of 1–5%. The measurement was conducted in triplicate.

From the amount of methane measured in the gas phase, the amount of dissolved methane in the permeate was calculated as described by Souza et al. [7]. The deviation of the dissolved methane was ±1.34 mg/L.

#### 2.3.7. Microbial Community

For the analysis of the microbial community, fresh samples were taken at the end of the experiment. They were centrifuged at 3068× *g* for 30 min and subsequently frozen and thawed three times to break up the cell walls. The DNA was extracted using a FastDNA™ SPIN Kit for Soil (MP Biomedicals Germany GmbH, 37269 Eschwege, Germany) according to the manufacturer's instructions.

To sequence the V4 region of the 16S rRNA gene, two-step, Nextera-barcoded PCR libraries using the primer pair 515F (5'-GTGYCAGCMGCCGCGGTAA-3') and 806R (5'-GGACTACNVTGGGTWTCTAAT-3') were applied [28]. Subsequently, the PCR libraries were sequenced on an Illumina NovaSeq 6000 platform using an SP 500 cycles kit (Illumina, Inc., San Diego, CA 92122, USA). The raw reads were uploaded to the NCBI Sequence Read Archive (SRA) under the BioProject accession number PRJNA1198955 [29].

The produced paired-end reads which passed Illumina's chastity filter were subject to de-multiplexing and trimming of Illumina adaptor residuals using Illumina's bcl2fastq software (version v2.20.0.422). The quality of the reads was checked with the software FastQC (version 0.11.8) [30], and low-quality reads (below average Q-score of 24 or uncalled bases "N") were removed from further analysis. The V4 primers were trimmed from the reads with the software cutadapt (version v3.2) [31]. Paired-end reads were discarded if the primer could not be trimmed. Trimmed forward and reverse reads of each paired-end read were merged using the software USEARCH (version 11.0.667) [32]. Merged reads that contained ambiguous bases or were outliers with respect to the expected amplicon size distribution were also discarded. The surviving reads were denoised using the UNOISE algorithm [33] implemented in USEARCH to form zero-radius OTUs (zOTUs). The resulting zOTU abundance table was then filtered for possible barcode bleed-in contaminations using the UNCROSS algorithm [34]. The zOTU sequences were compared to the reference sequences of the NCBI RefSeq Targeted Loci database provided by <https://www.ncbi.nlm.nih.gov/refseq/targetedloci/>, accessed on 29 December 2024. Taxa were predicted, and their confidences were calculated using the SINTAX algorithm [35] implemented in USEARCH.

Library construction, sequencing, and data analysis described above were performed by Microsynth AG (Balgach, Switzerland).

The reads were normalised with the Total Sum Squares (TSS) method using the package vegan (version 2.6-8) [36] in R (version 4.4.2) [37].

### 2.3.8. Data Processing and Visualisation

The data were processed for visualisation in R using the packages dplyr (1.1.4), tidyr (1.3.1), forcats (1.0.0), ggplot2 (3.5.1), and ggh4x (0.2.8).

## 3. Results and Discussion

### 3.1. Wastewater Composition

Prior to utilising the meat-processing wastewater as the substrate, an in-depth analysis of its composition was performed. The summarised results of the chemical analysis of all wastewater lots (average, standard deviation, minimum and maximum value) carried out over the course of the experiment are presented in Table 1. The characteristics of the wastewater exhibited fluctuations, particularly in pH, COD, and TS values, as illustrated by the standard deviation. The wastewater composition aligns well with the values found in the literature [38], although they comprise a considerable range [39].

The analysis of the samples taken continuously from the barrels during feeding (see Table 1, second column: 'feed') revealed a gradual change in the substrate composition. Compared to the data of the fresh wastewater (see Table 1, first column: 'wastewater'), the VFA were elevated, the TKN had almost entirely been converted into ammonium, and the average COD had decreased, all due to aerobic microbial activity in the feed storage barrel. This effect was not preventable and represents the actual practice in the field. Therefore, the effect was monitored and acknowledged.

Table 1 also provides the analytical data for the anaerobic reactor. The data show that the increase in the organic loading rate (OLR) did not lead to an overload of the system, resulting in eventual negative impacts. The pH was always within stable limits between 6.71 and 7.44, and the volatile fatty acid content never exceeded 371 mg/l. This is explicitly important for AnMBR systems, as in contrast to particulate organic matter, the VFA are not retained within the reactor and are washed out with the permeate. This is also reflected by the VFA content of the permeate, which displayed similar values. The TS in the reactor increased from 0.8% to 2.68%, which is a 3.35-fold increase, whereas the VS increased

6.7-fold from 0.18% to 1.21%. The higher accumulation rate of organic material can be explained by the propagation of microbes or the retention of undegraded organic matter. The growth of biomass in the reactor is also indicated by the increase in organic N (TKN minus NH<sub>4</sub>-N) from 0.31 up to 1.15 g/kg toward the end. Nevertheless, the N accumulation within the reactor was generally very low, and the TKN of the feed and the permeate were almost congruent. The original wastewater contained only a small share of the TKN in the form of NH<sub>4</sub>-N, on average 0.02 g/kg NH<sub>4</sub>-N. As explained above, in the feed, this share increased with storage time. NH<sub>4</sub>-N levels in the reactor and the permeate were similar, as ammonium is a dissolved molecule passing the membrane barrier.

**Table 1.** Characterisation of the wastewater used as substrate, the feed, the reactor content, and the permeate during the continuous feeding experiment.

		Wastewater	Feed	Reactor	Permeate
pH (-)	Min.	6.32	6.46	6.71	6.61
	Avg.	7.42 ± 1.09	7.28 ± 0.47	7.15 ± 0.21	7.17 ± 0.27
	Max	9.05	7.89	7.44	7.50
VFA (mg/L)	Min.	48.16	14.85	0.00	13.84
	Avg.	129.34 ± 82.91	632.79 ± 504.56	148.05 ± 154.11	139.00 ± 148.17
	Max	411.45	1204.99	371.31	368.49
COD (g/kg)	Min.	2.67	0.68	1.84	0.00
	Avg.	4.52 ± 1.29	2.83 ± 1.13	19.66 ± 20.28	0.90 ± 1.23
	Max	6.98	4.46	69.94	4.44
TS (%)	Min.	0.54	0.53	0.80	0.43
	Avg.	0.87 ± 0.22	0.79 ± 0.23	1.61 ± 0.65	0.64 ± 0.18
	Max	1.40	1.21	2.68	1.00
VS (%)	Min.	0.18	0.06	0.18	0.01
	Avg.	0.27 ± 0.05	0.18 ± 0.08	0.66 ± 0.35	0.05 ± 0.03
	Max	0.34	0.29	1.21	0.11
TKN (g/kg)	Min.	0.14	0.18	0.31	0.15
	Avg.	0.26 ± 0.06	0.28 ± 0.15	0.71 ± 0.27	0.21 ± 0.06
	Max	0.33	0.69	1.15	0.33
NH <sub>4</sub> -N (g/kg)	Min.	0.01	0.02	0.17	0.15
	Avg.	0.02 ± 0.01	0.21 ± 0.35	0.25 ± 0.07	0.21 ± 0.05
	Max	0.03	1.27	0.39	0.32
PO <sub>4</sub> -P (mg/L)	Min.		205.03		156.90
	Avg.		245.07 ± 22.56		211.79 ± 42.50
	Max		265.00		276.13

The phosphate concentrations in the feed and permeate were intermittently measured. The results indicate that its majority was channelled through the reactor and found in the permeate. Only small amounts are retained due to biomass growth.

The most notable characteristic of the substrate compared to other effluents from the meat industry, for example, slaughterhouse wastewater, is the elevated salt concentration [11,40]. This is reflected by the high conductivity, which averaged 3.9 ± 2.1 mS/cm, with a minimum of 1.72 and a maximum of 7.92 observed in hourly samples taken over 24 h. For comparison, the conductivity of municipal wastewater is usually in a range of 0.5 to 2.5 mS/cm [41]. The average conductivity corresponds to approximately 2.5 mg/L of dissolved salts, making it about 7.8% as saline as typical seawater [42–45]. The reactor conductivity increased from a minimum of 5.41 mS/cm to a maximum of 15.83 mS/cm over the course of the experiment with an average of 9.78 ± 2.3 mS/cm. Accumulated



particles and biomass also contribute to the conductivity. Such high conductivities of up to 16 mS/cm have also been reported in other studies of biogas plants [46]. To further characterise the salt content of the wastewater, it was assessed by measuring the anions with an ion chromatography system (Table 2).

**Table 2.** Ash content of the wastewater and salt composition determined using ion chromatography.

	Ash Content in TS [%]	Content of Anions in Ash [%]				% Anions in Ash
		Chloride	Nitrate	Phosphate	Sulphate	
Min.	57.4	44.9	-	3.4	1.0	49.8
Avg.	64.9 ± 5.7	58.7 ± 12.2	-	4.8 ± 2.1	1.1 ± 0.1	63.1 ± 11.7
Max.	70.7	71.2	-	7.2	1.1	74.7

It was determined that over 50% of the TS in the wastewater consist of ash, with nearly 60% of the ash being chloride, 5% phosphate, and 1% sulphate. Nitrate levels were below the detection limit. Various salts are used in meat products to serve different functional roles, including the regulation of moisture content and the enhancement of stability and shelf life. As these results show, part of the utilised salts end up in the wastewater. These elevated salt levels may pose challenges to microbial activity and inhibit microorganisms during anaerobic digestion of the wastewater. Despite the obvious importance of different ions in general in cell processes [47], bacteria are especially sensitive to osmotic and ionic changes, which makes salt concentration and ionic composition particularly important. High salt concentrations impose stress by increasing the osmotic pressure and the decrease in cell volume due to water loss through the membrane. This leads to concentration effects in the cell and ultimately harms the cell. But anions also supply cells with important elements, mainly sulphur, nitrogen, and phosphorous. For example, sulphate can act as an essential nutrient but at high concentrations as an osmotic stressor. After phosphate, sulphate is the second most abundant soluble oxyanion inside bacterial cells [48]. Furthermore, sulphur accounts for between 0.9 and 1.4 percent of cell dry matter and plays an important role in cells as a component of various amino acids and enzymes [47]. The salt composition shows that it serves as a valuable source of phosphorus and sulphate. Additionally, a notable decrease in methane production at high salt concentrations has been shown in other studies, but moderately elevated salt levels benefit VFA production [49,50].

In addition to analysing the characteristics of wastewater, detailed examinations of fat extraction and quantification were conducted to enhance the understanding of volatile solids (VS) composition. The estimation of VS composition was vital, relying on fat content and protein calculations from total Kjeldahl nitrogen (TKN) to assess its impact on biogas production. Highlighted in Table 3, fat and protein constitute a significant portion of VS in the wastewater, crucial for predicting biogas and methane potential. A residual VS component, accounting for 13.6%, was presumed to be carbohydrates, completing the composition analysis for theoretical yield estimates. Theoretical biogas yield calculations were grounded in methodologies by Baserga and Rutzmoser, providing a quantified forecast based on VS composition.

Furthermore, to estimate the theoretical methane yield, BMP tests were performed with two different inocula. The BMP test with the standard inoculum resulted in a methane potential of 635 Nm<sup>3</sup>/t (VS) (see Figure A1 and Table A1), which is higher than the theoretical estimation of 573 Nm<sup>3</sup>/t (VS). For the COD, a methane yield of 272 Nm<sup>3</sup>/t (COD) was found, which corresponds to 78% of the theoretical maximum of 350 Nm<sup>3</sup>/t (COD). The remaining 22% of the COD potential were either not biodegradable or not degraded in the time frame of the test; this uncertainty should be kept in mind when assessing the results of the BMP tests. In the BMP test using AnMBR digestate as the inoculum, the methane

potentials were found to be 146 Nm<sup>3</sup>/t (COD) and 216 Nm<sup>3</sup>/t (VS) (see Figure A2 and Table A2). The substantial difference between the two BMP tests shows that, at this point, the standard inoculum was more suitable for the degradation of the organics of the wastewater. Unfortunately, this inoculum contained fibrous materials that would have clogged the channels of the filtration unit. Therefore, anaerobic sludge from a WWTP was used for reactor start-up to avoid this problem. To exclude inhibitory substances accumulating in the AnMBR, which could explain the substantially lower BMP values compared to the standard inoculum, fed-batch tests were conducted. Therefore, the BMP tests were fed with sucrose as an easily available substrate. The fed-batch test with the standard inoculum and the AnMBR inoculum yielded similar BMP results of approximately 300 Nm<sup>3</sup>/t (COD) and 370 Nm<sup>3</sup>/t (VS). Concluding from these findings, the enzymatic activity of both inocula was similar, and no inhibitory effect was causing the lower methane potential found for the AnMBR inoculum. It was concluded that the AnMBR inoculum had not yet adapted to the wastewater substrate, causing an insufficient degradation of the organic matter and, therefore, lower BMP results.

**Table 3.** Fractions of fat, protein, and carbohydrates of the wastewater VS and theoretical methane yield calculated based on Baserga and Rutzmoser [26,27].

VS Composition	% Extractable Fats	% Protein	% Carbohydrates	Sum
Average [%]	25.6 ± 11.6	60.8 ± 7.2	13.6	100
Max [%]	43.5	71.6	-	-
Min [%]	10.3	53.5	-	-
Th. biogas yield [m <sup>3</sup> /t (VS)]	320 ± 145	426 ± 50	107	853 ± 195
Th. methane yield [Nm <sup>3</sup> /t (VS)]	218 ± 99	302 ± 36	54	573 ± 135
Th. methane concentration [%]	68	71	50	67

To check the evolution of the AnMBR sludge performance, another BMP test was conducted using standard inoculum and AnMBR sludge sourced on day 29. The results are shown in Figures A5 and A6, showing similar results for the standard inoculum (Table A5) but an increased yield of 324 Nm<sup>3</sup>/t (COD) and 498 Nm<sup>3</sup>/t (VS) for the BMP test, with the AnMBR inoculum bypassing the standard inoculum (Table A6). The standard inoculum was additionally tested with a cellulose standard to ensure robustness of the tests (Figure A7 and Table A7). It was concluded that the initial microbial community of the AnMBR sludge had not adapted to the wastewater in the start-up phase, but over the course of the continuous experiment, the methane yield substantially increased due to its adaptation.

### 3.2. Continuous Experiment

#### 3.2.1. Feeding Strategy

The initial daily feeding rate was 6 kg, corresponding to an HRT of three days, as illustrated in Figure 2. This rate was maintained for a duration of three weeks to allow for the adaptation of the microbial community. Subsequently, the feed rate was elevated to 10 kg per day with a corresponding HRT of 1.8 days, followed by increases to 14 kg and ultimately 18 kg per day, with an HRT of ~1 day. Due to maintenance activities, feed exchanges, and membrane-cleaning procedures, deviations from the planned feed occurred. These maintenance activities for membrane cleaning are only feasible manually in a lab-scale system but could be avoided in a large-scale application by applying automated backflushing. Although membrane cleaning was necessary on days 13, 47, and 60, the feed application was still maintained continuously, thus resulting in a gradual increase over the course of the experiment, represented by the black line in Figure 2.

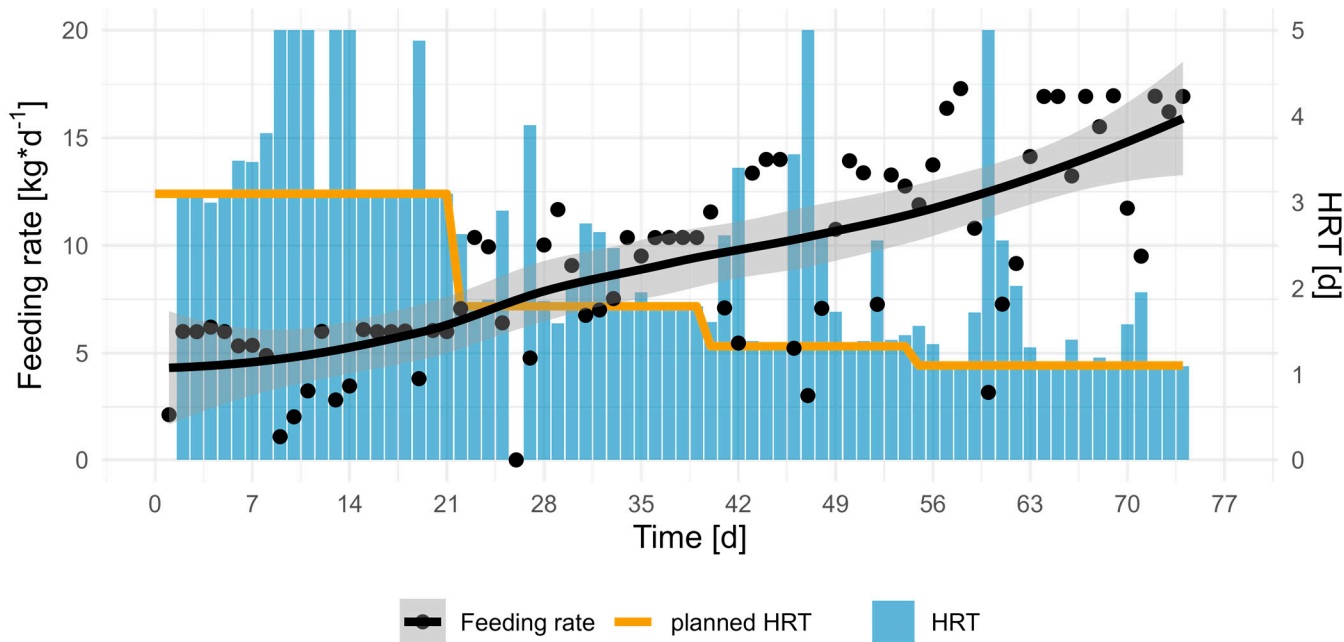


**Figure 2.** Wastewater-feeding rate and corresponding HRT over the course of the continuous experiment. Feeding rate illustrated as trend line (black line), calculated with R geom\_smooth function.

### 3.2.2. Biogas Production

Evidently, the increase in the feed rate coincided with a rise in OLR in terms of COD and VS. Given the fluctuations in the COD and VS content in the wastewater, the precise OLR depended on each lot of substrates. The fluctuations in OLR are shown in Figure 3, as well as the daily production of methane related to the working volume of the reactor.

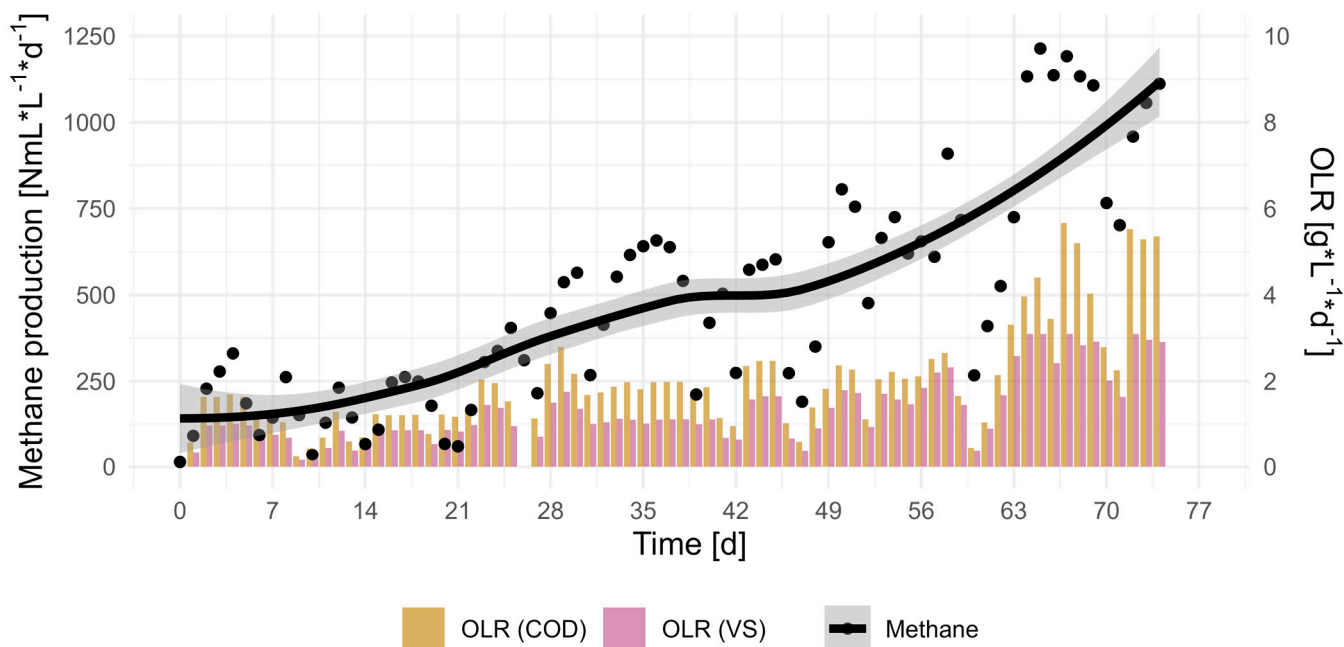


**Figure 3.** Daily methane production rate related to the reactors working volume corresponding to the increasing OLR. Methane production illustrated as trendline (black line), calculated with R geom\_smooth function.

Upon the introduction of a new barrel, daily methane production exhibited a gradual increase until the midpoint, followed by a decline. This phenomenon manifested itself as oscillations in daily methane production, attributed to the accumulation of fat deposits on the walls of the barrel and the ongoing aerobic decomposition within the barrel. Despite that, the results clearly demonstrate an overall increase in methane production in conjunction with increased feed supply and OLR.

The composition of the biogas was systematically monitored and is illustrated in Figure 4. The methane content remained consistently high, with an average of approximately 80%; correspondingly, the concentration of CO<sub>2</sub> was below 20%. The concentration of hydrogen sulphide demonstrated an upward trend in conjunction with increased OLR, reaching a peak of nearly 2000 ppm at the conclusion of the experiment. The hydrogen concentration within the biogas remained below 200 ppm; although, a slight increase was observed in the final two weeks with the application of the highest loading rate. No oxygen was detected throughout the experiment, confirming anaerobic conditions and no air contamination during sampling or feeding.

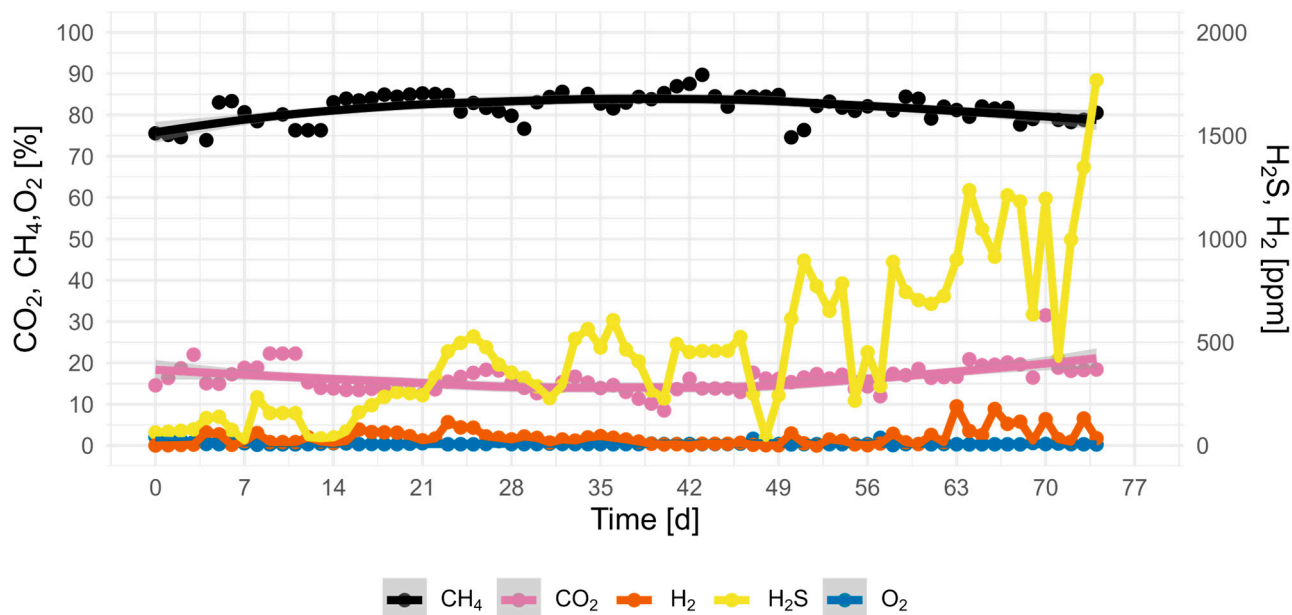


**Figure 4.** Biogas composition produced in the AnMBR during the continuous experiment.

The unusually high methane concentration can be explained by a washout effect of CO<sub>2</sub> with the permeate stream, as CO<sub>2</sub> dissolves more readily in water compared to methane. This was also found in other AnMBR studies [8,51,52]. These results suggest that the biogas obtained is particularly suitable for upgrading, as the methane concentration is already high compared to other reactor designs. Therefore, less effort would be required to achieve the quality necessary for injection into the gas grid.

The specific methane yield for COD and VS was derived from the standardised daily methane production and the applied OLR as the yield per COD and VS loaded. For the calculation of the yield removed, the organics lost with the permeate were subtracted from the feed concentrations. The yields were organised into three phases corresponding to three increasing average OLRs, as depicted in Figure 5. Phase 1 corresponds to an OLR of 0.71 gCOD/(L\*d), 0.65 gVS/(L\*d), and HRT of 3.4 days; phase 2 to 1.15 gCOD/(L\*d), 1.67 gVS/(L\*d), and HRT of 2.0 days; and phase 3 to 2.25 gCOD/(L\*d), 1.85 gVS/(L\*d), and HRT of 1.4 days.

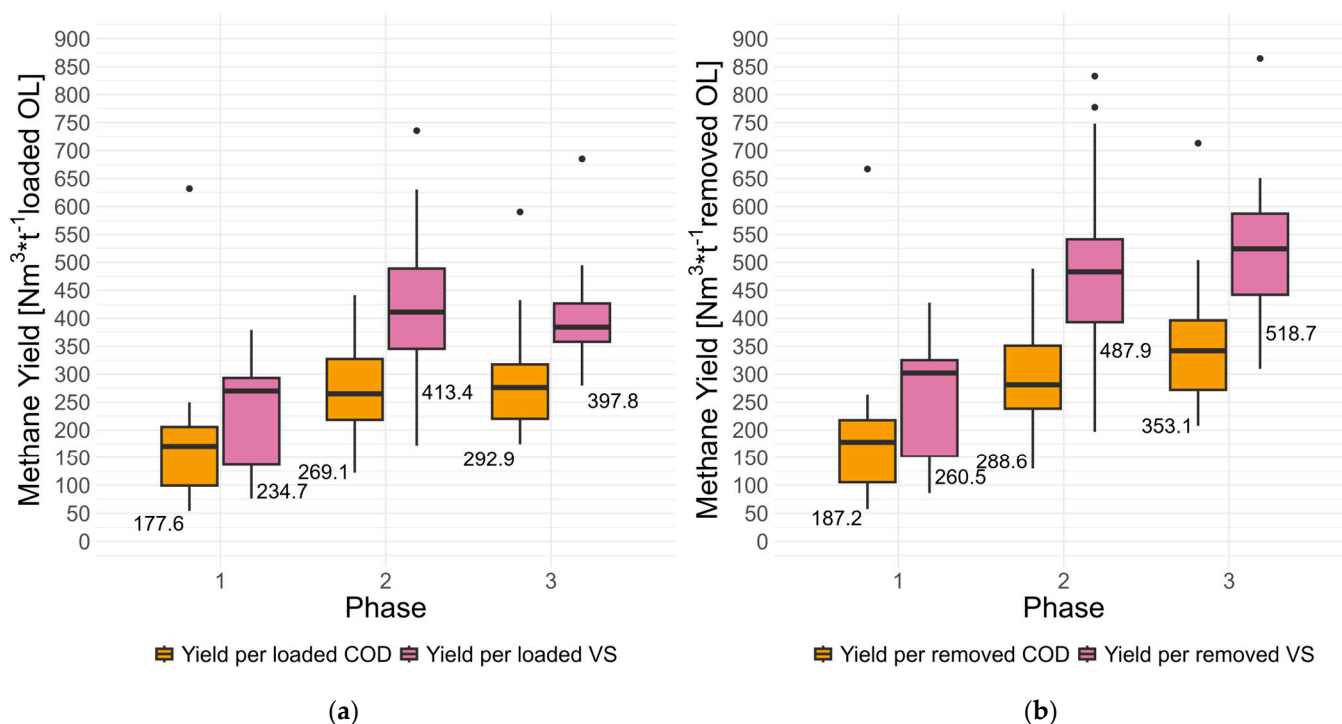


**Figure 5.** Methane yield at increasing organic loading rates for COD and VS. Phase 1 corresponds to an OLR of 0.71 gCOD/(L\*d), 0.65 gVS/(L\*d), and HRT of 3.4 days; phase 2 to 1.15 gCOD/(L\*d), 1.67 gVS/(L\*d), and HRT of 2.0 days; and phase 3 to 2.25 gCOD/(L\*d), 1.85 gVS/(L\*d), and HRT of 1.4 days. (a) Methane yield calculated per loaded organics. (b) Methane yield calculated per organics removed.

In phase 1, the methane yield per COD and VS loaded (Figure 5a) is comparable to the results of the biogas potential tests using the AnMBR inoculum (see Section 3.1), specifically  $178 \text{ Nm}^3/\text{t}$  (COD) and  $235 \text{ Nm}^3/\text{t}$  (VS) on average. And due to the high HRT and COD removal rates, the yield per COD and VS removed (Figure 5b) is only slightly higher. As the OLR increased over time, an increase in yield was observed in the yield loaded and removed. In phase 2, the yield was  $269 \text{ Nm}^3/\text{t}$  (COD) and  $413 \text{ Nm}^3/\text{t}$  (VS) on average but with a relatively high variance. The highest methane yield was achieved at the highest OLR in phase 3, reaching nearly  $293 \text{ Nm}^3/\text{t}$  (COD) and  $398 \text{ Nm}^3/\text{t}$  (VS) on average per organics loaded. This is lower compared to the predicted theoretically methane yield (Table 3), but the yields per removed organics with  $519 \text{ Nm}^3/\text{t}$  (VS) is close to the prediction of  $573 \text{ Nm}^3/\text{t}$  (VS). The  $353 \text{ Nm}^3/\text{t}$  (COD) removed is slightly above the theoretical maximum of 350 and indicates that the COD not lost with the permeate was efficiently converted to methane at this stage. In light of these data, it is important to mention the findings of Curtis et al., stating that the degradation of organics does not necessarily result in the formation of methane and that the energy contained in the molecules differs independently from the COD values [53]. Considering the fluctuations in substrate composition, this explains some inconsistency in the specific yields regarding COD and VS. However, the same general trend is evident, namely that the increase in the OLR and the progression over time are accompanied by an increase in the specific methane yield.

Overall, the difference between the yields loaded and removed increased with the increase in the organic loading rate because more dissolved organics were lost with the permeate due to the shorter HRT reducing the yields per organics loaded. The methane yield per COD loaded surpassed the BMP tests of  $272 \text{ Nm}^3/\text{t}$  (COD) with the standard inoculum. The batch test with the adapted AnMBR inoculum reached a higher yield of  $324 \text{ Nm}^3/\text{t}$  (COD), which is closer to the maximum yield per removed COD. The extent



of biodegradation in these BMP test must have been very high, since they reached similar yields as the AnMBR per removed organics. For the yield per VS, neither the yield per loaded nor the yield per removed organics reached the theoretical estimate of 573 Nm<sup>3</sup>/t (VS). The result of 519 Nm<sup>3</sup>/t(VS removed) is again close to the yield of the adapted AnMBR inoculum batch test of 498 Nm<sup>3</sup>/t (VS) and much higher compared to the yield of loaded VS reaching 398 Nm<sup>3</sup>/t (VS). The lower yields found for the loaded organics are not due to the degradability but due to the shorter HRT, leading to a greater loss of organics with the permeate. The methane yields found in the BMP tests and for the AnMBR for the organics removed are similar, since the BMP tests are run until most organics are degraded, and for the AnMBR, the lost organics are not considered for the yield. For the comparability to other systems, the yield per loaded organics remains the relevant parameter, even though the yield of the BMP tests is better comparable to the yield per removed contaminants.

### 3.2.3. Contaminant Removal and Water Recovery

The permeate from the ultrafiltration was analysed regularly (see Table 1, fourth column: ‘permeate’) and the average removal rates regarding the measured parameters compared to the feed were calculated. The COD experienced a reduction of 81.7%, whereas 69.8% of the VS was removed, although there was only a reduction of approximately 19.8% in the TS. TKN was reduced by 20.1%; however, due to the conversion of all nitrogen to dissolved ammonium, no ammonium removal was observed apart from the amount accumulated within the biomass. Furthermore, only 19.7% of the phosphorus was removed.

In Figure 6, the COD removal rates are shown broken down into three phases. The COD removal rate decreased with increasing OLR from 100% to 73% with an average OLR of 2.25 g/(L\*d). This shows that the average reduction in COD does not necessarily correspond to the overall effectiveness in terms of methane production.

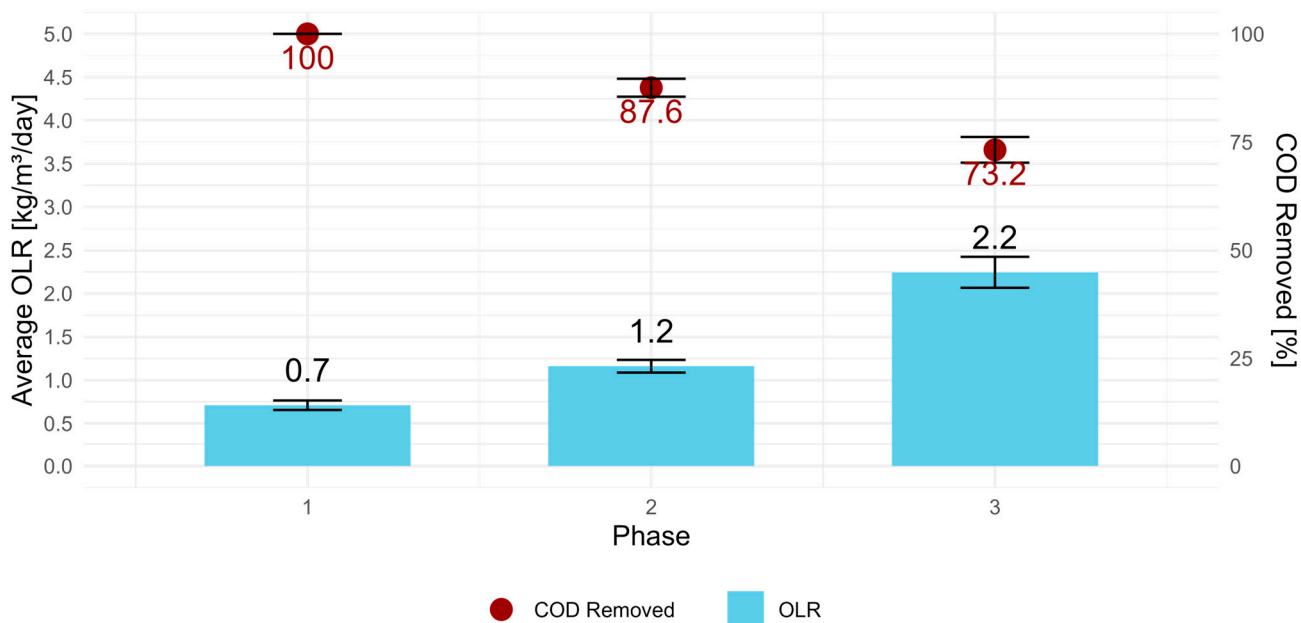


**Figure 6.** COD removal for each average OLR (COD). Phase 1 corresponds to an OLR of 0.71 gCOD/(L\*d) and HRT of 3.4 days; phase 2 to 1.15 gCOD/(L\*d) and HRT of 2.0 days; and phase 3 to 2.25 gCOD/(L\*d) and HRT of 1.4 days.

In general, the reported COD removal rates align with the range reported in other studies conducted on comparable systems [2]. Galib et al. reported an increase in the COD removal with an increase in the loading rate [39]. The observed decline in COD removal may be attributed to an excessively rapid increase in the OLR. When the increase

in OLR takes place faster than the growth rate of the required microorganisms, the current metabolic rate is insufficient to reduce the contaminants. The dissolved metabolites are washed out with the permeate, and hence, the reduction rate is reduced.

In comparison to Galib et al., a COD removal rate of 87.5% was reported at an OLR of 3.14 gCOD/(L\*d) compared to the removal rate of 73.2% found in this study at an OLR of 2.25 gCOD/(L\*d), but this was reached in 77 days, while Galib et al. accomplished the higher removal rate by keeping the same OLR for 75 days [39]. This indicates that the described AnMBR system adapted fast to increasing loads, and an optimised methane production is possible. But for consistently high permeate quality, the OLR has to be kept stable for a longer period of time.

In comparison, Whahaab et al. tested a UASB for the treatment of meat-processing wastewater, only reaching a COD removal rate of 51%. Even with the implementation of a subsequent aerobic step, a rotating biological contactor, they obtained only a COD removal rate of 81% although using a lower COD inflow concentration compared to this study [54]. This demonstrates that the AnMBR system is a well-suited system for the treatment of wastewater from the meat-processing industry as well as for the utilisation of the contained organics for efficient biogas production.

When comparing the relevant concentrations found in the permeate with the requirements of the Austrian legislation for direct discharge of wastewater from the meat industry [55], the COD, is on average, higher by a factor of 10 than the required 0.09 g/L, the NH<sub>4</sub>-N by a factor of 42 (required 0.005 g/L), and phosphorous by a factor of 211 (required 1 mg/L). Furthermore, when examining the total maximum chlorine levels of 0.4 mg/L, the permeate concentrations are likely too high according to the TS and ash content (Tables 1 and 2). An additional treatment step is needed if the water is supposed to be discharged or reused. Nanofiltration or reverse osmosis are potential post-treatment options that could be beneficially applied not only to further reduce contaminants, but also as a means of nutrient recovery.

This approach is supported by new concepts in wastewater treatment [56] that particularly aim at nutrient and energy recovery. It could contribute to the EU water reuse policy that has recently changed in light of the increasing draught risk and fresh water scarcity as well as the energy crisis and the human-made climate change [57]. In this context, it is important to see the tremendous improvements in energetic efficiency of membrane technology made in the past years. According to the forecast by Smith et al., net energy positive operation of AnMBRs is achievable in the near future [58].

When considering all this information, it remains challenging to formulate an economic statement. The costs for COD removal in a WWTP are estimated by Yapıcıoğlu et al. to be 726.6 and 65,520 €/m<sup>3</sup> of wastewater for design and operational conditions, respectively. Within the context of the water–energy nexus, wastewater reuse could be considered to reduce energy costs. These energy costs could potentially be reduced by approximately 49% if wastewater reuse were implemented in the plant. Thus, wastewater reuse is feasible, utilising advanced wastewater treatment methods such as membrane processes, adsorption, and oxidation processes, among others. Among these, the AnMBR process may be preferred as a reuse technology due to its ability to produce a higher effluent quality [15]. Pan et al. (2018) conducted a similar study focusing on the water–energy nexus, recommending wastewater reuse for cooling water [59]. As shown, this technology is also applicable for the treatment of wastewater from meat processing. Sludge treatment results in high operational costs in WWTPs. The AnMBR system is considered to be a nearly zero-sludge system, which would consequently lower operational costs if implemented.

The energy demands of the AnMBR in general include requirements for liquid recirculation, biogas scouring, and permeation. An energy consumption of 0.40 kWh/m<sup>3</sup> was

calculated by Galib et al. The authors achieved a net energy benefit of 0.13–5.1 kWh/m<sup>3</sup> with their system and demonstrated that AnMBRs utilised for treating meat-processing wastewater could potentially serve as an energy-independent wastewater treatment technology, assuming an energy conversion efficiency of approximately 40% from thermal to electrical energy [39].

In this context, Smith et al. compared different systems, namely high-rate activated sludge with anaerobic digestion (HRAS+AD), conventional activated sludge with anaerobic digestion (CAS+AD), and aerobic membrane bioreactor with anaerobic digestion (AeMBR+AD) for high-strength domestic wastewater treatment. They stated the AnMBR exhibited a 15% higher net energy recovery compared to HRAS+AD. The lifecycle costs of energy recovery systems are notably lower compared to conventional systems. As technological advancements in AnMBR continue, capital and operational costs will further decrease. And the increase in flux from 10 to 20 L/(m<sup>2</sup>·h) results in a reduction in capital costs by 46%. Assuming constant chemical and energy use per unit membrane area, the operational costs related to membrane cleaning and fouling control will also decrease with increasing flux. Consequently, doubling the flux reduces the lifecycle AnMBR costs by approximately 12–13%, leading to a lower lifecycle cost compared to HRAS+AD. In particular, HRAS+AD was the only system to achieve a positive net energy balance, but with future advances, the energy competitiveness of the AnMBR could be achieved. Especially, fouling control comprised 86% of the total energy requirements [58].

Another challenge that limits the economic efficiency and sustainability of AnMBRs is the loss of methane as dissolved methane with the permeate.

#### 3.2.4. Dissolved Methane

One of the known drawbacks of the AnMBR system, but also other systems with high hydraulic loading rates as UASB reactors, is the dissolution of certain methane quantities which are lost with the permeate stream [60]. Methane loss with the permeate poses a problem not only for process efficiency and economic viability but also due to its global warming potential, which is 21 times higher compared to CO<sub>2</sub> [61].

The dissolved methane concentration is influenced by many factors like the temperature, pH, salt concentration, methane concentration, biogas production, and the HRT. To quantify the potential loss of methane in this study, the dissolved methane concentration was measured at the different HRT/OLR and compared to the theoretical concentration according to Henry law [62], shown in Figure 7. The total methane loss was derived from the measured concentrations of dissolved methane and the permeate production.

With the increase in OLR and permeate production, the daily methane production also increased correspondingly. The measured dissolved methane increased from 7.5 mg/L up to 10 mg/L, which is clearly lower than the theoretical value. At the lowest OLR, less than half of the theoretically expected dissolved methane was measured.

Combining the dissolved methane data with the permeate flow reveals substantial methane loss particularly at a lower HRT. However, even at the maximum permeate production of about 14 L/day, the methane loss per day was only 130 mg/d, corresponding to 0.02 m<sup>3</sup>/d methane at standard conditions. At this stage, the daily methane production of 12 L/d represents 1.3% of the total daily methane production. The observed values are much lower compared to other studies, where higher dissolved-methane concentrations have been found. Concentrations in the permeate as high as 50 mg/L [39,63,64] and a methane loss of almost 80% [64,65] are reported, caused by an oversaturation effect through mass transfer inhibition, as described in detail by Yeo et al. [64]. The observed low concentrations can be attributed to the increased salt content and elevated temperature, which reduces methane solubility, as demonstrated by Yin et al. [60].

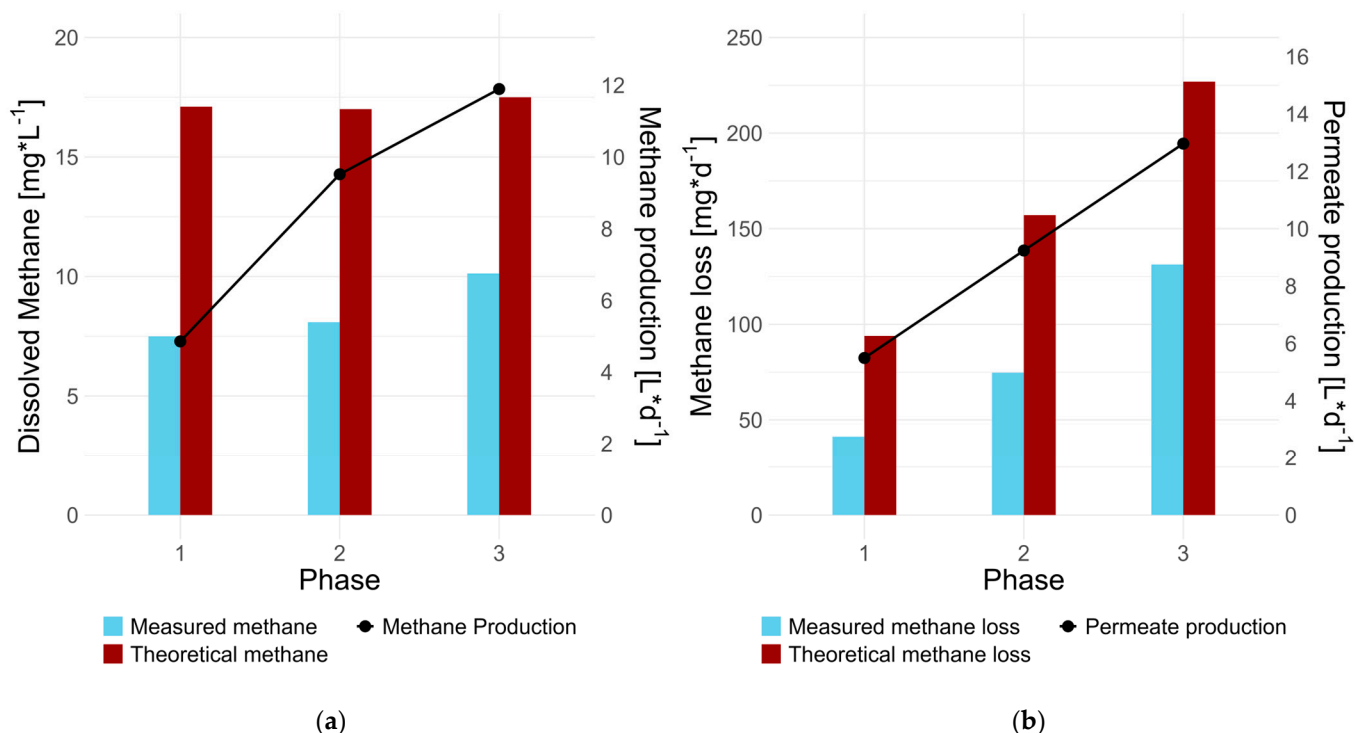


**Figure 7.** Dissolved methane and methane loss: (a) measured and calculated theoretical methane concentration in the permeate sorted by three different OLR and corresponding HRT and additionally the corresponding methane production per day; (b) calculated total methane loss from the theoretical and measured methane concentrations and the daily permeate volume sorted by three different OLRs, corresponding HRTs, and, additionally, the corresponding permeate production per day. Phase 1: OLR 0.71 gCOD/(L·d), 0.65 gVS/(L·d), and HRT of 3.4 days; phase 2: 1.15 gCOD/(L·d), 1.67 gVS/(L·d), and HRT of 2.0 days; phase 3: 2.25 gCOD/(L·d), 1.85 gVS/(L·d), and HRT of 1.4 days.

While elevated salt concentrations might enhance the process by lowering the dissolved methane concentration in the permeate, they can adversely affect the microbial community and its efficacy in biomethane production.

### 3.3. Microbial Community

The composition of the microbial community was analysed at the end of the experiment to evaluate which microorganisms can adapt to the substrate. As the wastewater used in this study has high fat and salt content, this shall help to identify groups of microorganisms that can deal with such stress factors. On the other hand, potentially harmful microorganisms can be detected. The dominant bacterial classes (class abundance > 2%) and the dominant archaeal orders (order abundance > 0.2%) are shown in Figure 8.

The most abundant phylum is Chloroflexota (35% of the community), made up exclusively of the class Anaerolineae. Chloroflexota have been reported to utilise carbohydrates and proteins for the production of acetate and hydrogen [8]. As described above, the membrane of the AnMBR had to be cleaned regularly. The high abundance of Chloroflexota could be a primary contributing factor on that problem, as they can promote biofouling by EPS production [4,8]. Chloroflexota are followed by the phylum Bacillota (formerly named Firmicutes; 22%), with the most dominant class Clostridia. These have been reported to be present in reactors fed with high fat content [66], as well as reactors fed with slaughterhouse waste [67] and with elevated salt and oil concentrations [50]. They are involved in a number of important pathways in the biogas process: They degrade lipids and proteins through extracellular enzymes and produce VFAs and hydrogen [8,66,67]. Both of these phyla are typical for anaerobic digestion communities and are often the major groups in biogas

reactors [8]. The ratio found in the sample (more Chloroflexota than Bacillota) might be caused by the high OLR applied at the end of the continuous experiment [8].

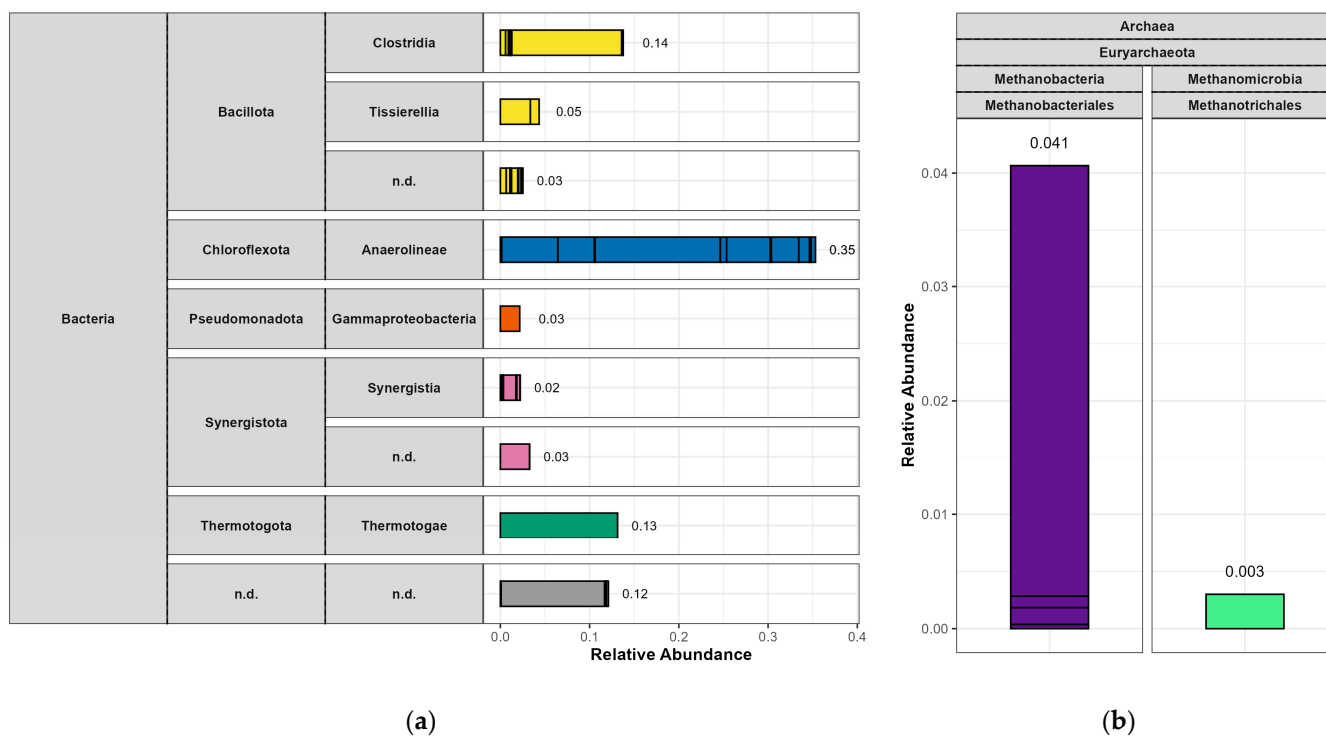


**Figure 8.** Microbial community composition in the AnMBR. Confidence threshold was set at 70%; at a lower confidence, the taxa are labelled ‘n.d.’. (a) Bacteria at phylum and class level. Only classes with an abundance of at least 2% are shown; (b) archaea at phylum, class, and order level. Only orders with an abundance of at least 0.2% are shown.

Other bacterial phyla found are Thermotogota (13%), Synergistota (5%), and Pseudomonadota (formerly named Proteobacteria; 3%), which are all typical members of the microbial community found in anaerobic digestion [50]. Synergistota are involved in the production of acetate, hydrogen, and CO<sub>2</sub> from long-chain fatty acids [50], thus degrading the compounds of the substrate to metabolites used by methanogenic archaea. The unusually low abundance of Pseudomonadota might be caused by the properties of the meat-processing wastewater, i.e., the low carbohydrate and high fat content.

Archaea account for 4% of the microbial community. The two major groups of archaea in anaerobic digestion systems are acetoclastic methanogens, which utilise acetate for methane production, and hydrogenotrophic methanogens, which produce methane from H<sub>2</sub> and CO<sub>2</sub> [49,67]. The archaea found in this AnMBR are almost exclusively made up of Methanobacteria and, a small part, of Methanomicrobia. Both groups are classified as hydrogenotrophic methanogens [67]. Only traces of acetoclastic methanogens were found, which might again be due to the properties of the used substrate, as indicated by several studies: Hydrogenotrophic methanogens are more resistant to environmental stress [49] and make up most of the archaeal community in biogas reactors utilising slaughterhouse waste and substrates with high oil and/or salt content [50,67]. Methanobacteria live in a syntrophic relationship with hydrogen-producing bacteria; members of the phylum Bacillota, for example, can produce and further degrade acetate to CO<sub>2</sub> and H<sub>2</sub>, serving as the substrate for methane production by Methanobacteria [50].



## 4. Conclusions

In conclusion, the AnMBR system exhibited a rapid and stable start-up and demonstrated the capacity to handle increasing OLRs effectively. Biogas production increased with higher feed rates, although this was accompanied by a reduction in COD removal efficiency, from 100% to 73%. The methane yield per organics removed increased matching the BMP test results, but the difference to the yield per loaded organics increased with the OLR because of the lower reduction rates. Although the system is suitable for biogas production from meat-processing wastewater, effluent quality needs additional treatment to meet regulatory standards. Dissolved methane losses remained minimal at 1.3% of daily production due to the reactor's high temperature and salting-out effects. For the biogas sector, it is crucial to gain more knowledge on the relationship between process parameters (e.g., substrate composition) and the microbial community to better respond to the demands of microbes, making microbe groups that can best deal with a specific wastewater outcompete others, and thus optimising the biogas yield and wastewater treatment. The characteristics of the microbial community, including stress resistance and hydrogenotrophic methane production, align with those of reactors processing substrates with a high fat and salt content. While this suggests potential for the treatment of high-strength wastewaters, specific measures to mitigate their impact on membrane fouling need further investigation. The demonstrated integration of biogas production and wastewater treatment presents opportunities for a broader application in food-processing sectors with high volumes of wastewater. Co-digestion with alternative waste streams and pilot studies could further validate and refine this approach, promoting sustainable water and waste management practices in centralised food processing operations.

**Author Contributions:** Conceptualisation, F.H. and L.B.; methodology, F.H., L.B., W.G., W.F.; validation, W.G. and W.F.; formal analysis, F.H., L.B.; investigation, F.H.; resources, F.H., W.G.; data curation, F.H., L.B.; writing—original draft preparation, F.H.; writing—review and editing, F.H., L.B., W.G., and W.F.; visualisation, F.H. and L.B.; supervision, W.F.; project administration, W.G.; funding acquisition, W.G. All authors have read and agreed to the published version of the manuscript.

**Funding:** This research was funded by the European Commission under Horizon Europe (HORIZON), Grant agreement ID: 101058426, <https://doi.org/10.3030/101058426>.

**Institutional Review Board Statement:** Not applicable.

**Informed Consent Statement:** Not applicable.

**Data Availability Statement:** The raw data supporting the conclusions of this article will be made available by the authors on request. The raw DNA reads were uploaded to the NCBI Sequence Read Archive (SRA) under the BioProject accession number PRJNA1198955 [29].

**Acknowledgments:** The authors gratefully acknowledge the contribution of the SYMSITES cooperation partners for providing materials and samples. We also thank BOKU University and the Institute of Environmental Biotechnology for access to facilities and equipment. Special thanks to Ivana Mihajlovic and Marion Sumetzberger-Hasinger for their support with analysis and devices, and to Günther Bochmann for his significant role in securing funding. We appreciate Lukas Hässmann's diligent execution of his bachelor thesis and data acquisition. The Writefull Word add-in was used for language improvements, spelling, and grammar checks.

**Conflicts of Interest:** The co-author Lisa Bauer was employed by the company BEST-Bioenergy and Sustainable Technologies GmbH. The remaining authors declare that the research was conducted in the absence of any commercial or financial relationships that could be construed as a potential conflict of interest.

## Appendix A

### Appendix A.1. Batch Tests (BMP Tests)—Implementation and Execution in Detail

Batch tests were carried out in triplicate to estimate the theoretically achievable methane yield per employed wastewater in the AnMBR. The testing of wastewater was difficult because of the very low COD concentrations and with it the associated higher required substrate amounts resulting in a higher dilution of the inocula. This obstacle was overcome for the standard inoculum test by mixing an anaerobic digestate from a biogas plant and a WWTP at a ratio of 1:1, resulting in a TS of 3.5%. The substrate and inoculum were mixed to reach an inoculum-VS-to-substrate-VS ratio of 0.3–0.5. The substrate-to-inoculum ratio (SIR) was set to 0.4 for the batch tests. For the AnMBR inoculum tests, higher amounts of inoculum were used to reach the same SIR.

Additionally, to the batch tests for the BMP fed-batch tests were also carried out to test for inhibition because of detergents, salts, or other components of the wastewater stream of the AnMBR sludge. After the batch tests were finished and no biogas was produced anymore, the same batch tests were fed with sucrose (SIR = 0.18) to test if the AnMBR sludge was slower or less effective in the degradation of an easily degradable substrate.

### Appendix A.2. Results of the Batch Tests and Inhibition Experiments

The first batch test of wastewater with standard inoculum is represented in Figure A1, displaying a gradual degradation and no lag phase. The average results are shown in Table A1 with a methane yield  $V(\text{CH}_4)$  in  $\text{Nm}^3/\text{t COD}$  of 272 and 635  $V(\text{CH}_4)$  in  $\text{Nm}^3/\text{t VS}$ .

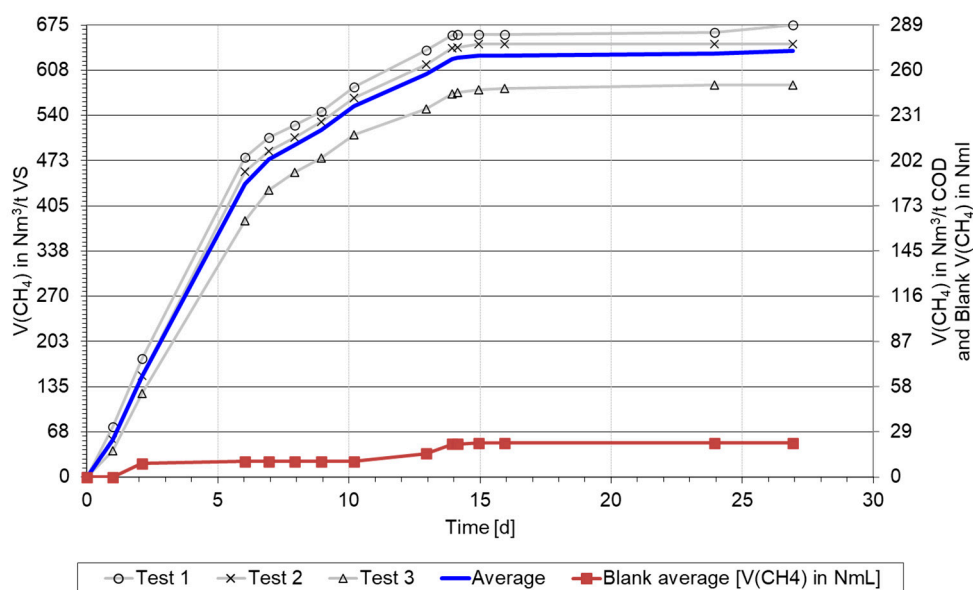


**Figure A1.** Graphical representation of the batch test results of wastewater as the substrate and standard inoculum (SIR = 0.4).

**Table A1.** The batch test results of wastewater as the substrate and standard inoculum (SIR = 0.4).

	Average	Minimum	Maximum
$Y(\text{CH}_4)$ in $\text{Nm}^3/\text{t}(\text{FM})$	1.0	0.8	1.1
$Y(\text{CH}_4)$ in $\text{Nm}^3/\text{t}(\text{COD})$	272	227.9	317.0
$Y(\text{CH}_4)$ in $\text{Nm}^3/\text{t}(\text{VS})$	635	532.6	738.7

The batch test of wastewater with inoculum sourced from the AnMBR at the beginning of the continuous feeding experiment is represented in Figure A2, also displaying a gradual

degradation and no lag phase. However, the average results shown in Table A2 with a methane yield  $V(\text{CH}_4)$  in  $\text{Nm}^3/\text{t}$  COD of 146 and 216  $V(\text{CH}_4)$  in  $\text{Nm}^3/\text{t}$  VS are dramatically lower when using the AnMBR content as inoculum.

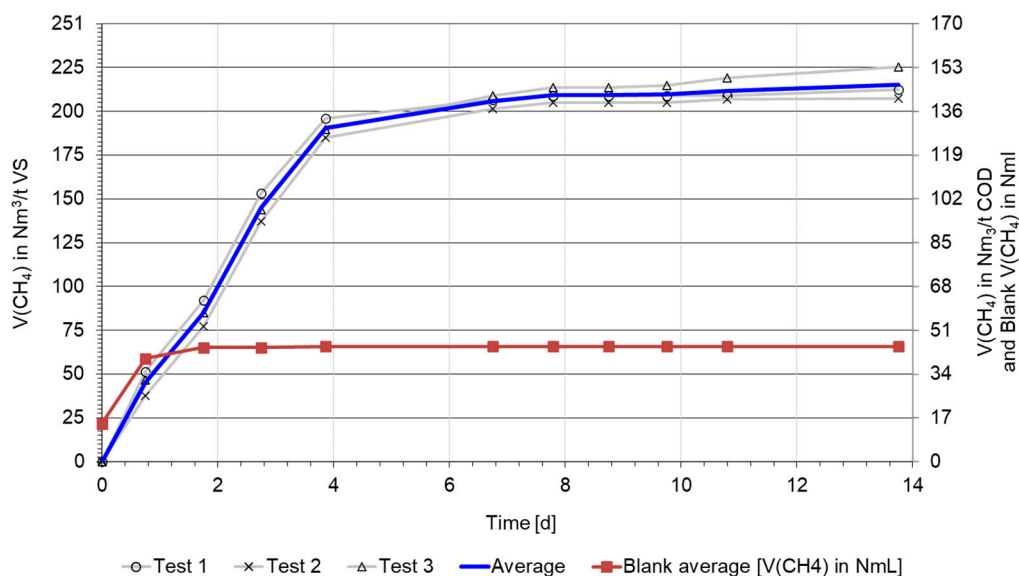


**Figure A2.** Graphical representation of the batch test results of wastewater and AnMBR inoculum (SIR = 0.4).

**Table A2.** Table of the batch test results of batch test results of wastewater and AnMBR inoculum (SIR = 0.4).

	Average	Minimum	Maximum
$Y(\text{CH}_4)$ in $\text{Nm}^3/\text{t}(\text{FM})$	0.3	0.3	0.4
$Y(\text{CH}_4)$ in $\text{Nm}^3/\text{t}$ (COD)	146	122.4	170.3
$Y(\text{CH}_4)$ in $\text{Nm}^3/\text{t}$ (VS)	216	180.6	250.5

To test if the big difference in the yield of the BMP tests between the two different inocula resulted from an accumulation of inhibitory substances in the AnMBR reactor, the batch tests were used in a subsequent fed-batch experiment after biogas production had ceased. Sucrose was fed to the batches at a 0.18 substrate-VS to-inoculum-VS ratio. This low ratio was selected because of the very fast degradability of sucrose, which could lead to higher ratios of unwanted fast biogas production and botched test results.

The fed-batch results of the standard inoculum fed with sucrose at a VS ratio of 0.18 is represented in Figure A3. After a short lag phase at the first day, the sucrose was degraded within a week. The yields are displayed in Table A3 with a methane yield  $V(\text{CH}_4)$  in  $\text{Nm}^3/\text{t}$  COD of 313 and 382  $V(\text{CH}_4)$  in  $\text{Nm}^3/\text{t}$  VS.

**Table A3.** Results of the fed-batch results of the standard inoculum and sucrose as the substrate (SIR = 0.18).

	Average	Minimum	Maximum
$Y(\text{CH}_4)$ in $\text{Nm}^3/\text{t}(\text{FM})$	344.0	288.9	399.2
$Y(\text{CH}_4)$ in $\text{Nm}^3/\text{t}$ (COD)	313	261.8	364.1
$Y(\text{CH}_4)$ in $\text{Nm}^3/\text{t}$ (VS)	382	320.4	444.3

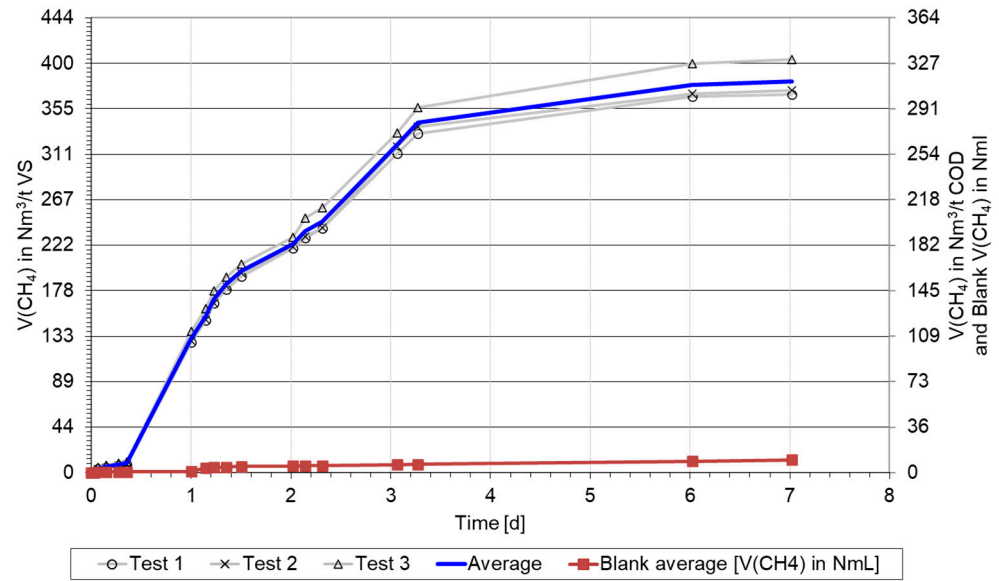


**Figure A3.** Graphical representation of the fed-batch results of the standard inoculum and sucrose as the substrate (SIR = 0.18).

The batch test with AnMBR inoculum was used for a fed-batch as well at a VS ratio of 0.18, represented in Figure A4. After a short lag phase at the first day, the sucrose was degraded within a week. The biogas evolution graph of both inocula fed with sucrose look very similar, which indicates a similarly good degradation. The yields are displayed in Table A4 with a methane yield  $V(\text{CH}_4)$  in  $\text{Nm}^3/\text{t COD}$  of 301 and 368  $V(\text{CH}_4)$  in  $\text{Nm}^3/\text{t VS}$ . The yields for sucrose with the AnMBR inoculum are slightly less but within the fluctuation range and therefore neglectable. This shows that no inhibitory substances accumulate in the AnMBR because of the UF process. Thus, the differing initial BMP test results in comparison to the standard inoculum must have a different cause. An explanation could be the poorer adaptation of the microbial community in the AnMBR to the new substrate, as it was sourced from a wastewater treatment plant, while the standard inoculum is a mixture with sludge from a biogas plant, which is used to a broader span of substrates.

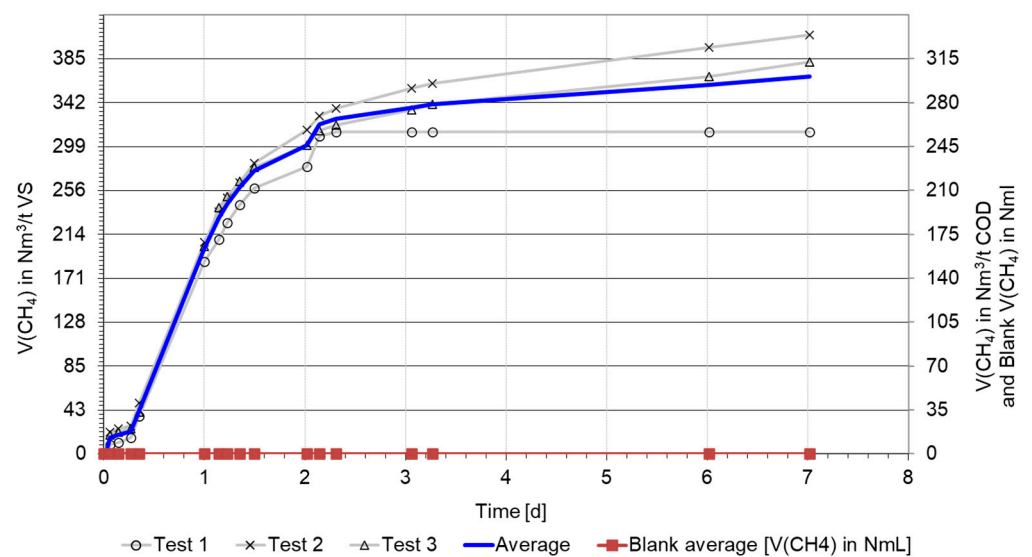


**Figure A4.** Graphical representation of the fed-batch with the AnMBR inoculum batch and sucrose as the substrate (SIR = 0.18).

**Table A4.** Results of the fed-batch with the AnMBR inoculum batch and sucrose as the substrate (SIR = 0.18).

	Average	Minimum	Maximum
Y(CH <sub>4</sub> ) in Nm <sup>3</sup> /t(FM)	330.9	277.8	383.9
Y(CH <sub>4</sub> ) in Nm <sup>3</sup> /t (COD)	301	251.8	350.2
Y(CH <sub>4</sub> ) in Nm <sup>3</sup> /t (VS)	368	308.1	427.4

To test this hypothesis, batch tests were repeated at the same conditions as before, but the AnMBR sludge was sourced from the reactor at a later stage of the continuous feeding experiment (day 29). The withdrawn amount of the AnMBR was replenished with feed.

The results of the second batch test with wastewater and standard inoculum is shown in Figure A5. The degradation appears to be not as smooth as in the first batch test, but in both batch tests, the biogas production ceased after two weeks and reached similar yields. The yields of the second batch test with the standard inoculum are represented in Table A5, with a methane yield of 274 Nm<sup>3</sup>/t (COD) and 421 Nm<sup>3</sup>/t (VS), which is almost identical to those presented in Table A1.

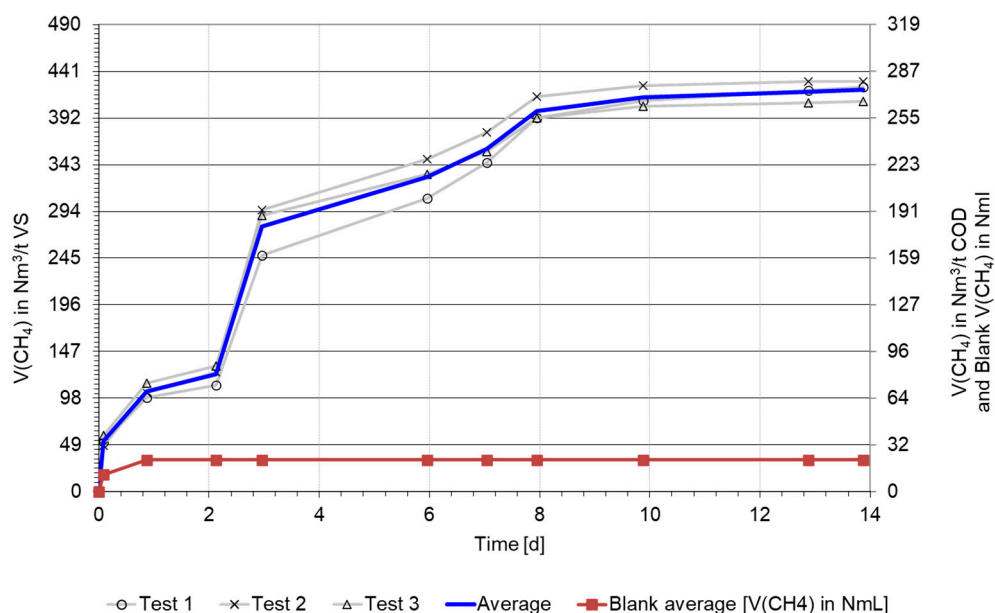


**Figure A5.** Graphical representation of the results of the second batch test with wastewater and the standard inoculum (SIR = 0.4).

**Table A5.** Table of the batch test results of the second batch test with wastewater and the standard inoculum (SIR = 0.4).

	Average	Minimum	Maximum
Y(CH <sub>4</sub> ) in Nm <sup>3</sup> /t(FM)	0.5	0.5	0.6
Y(CH <sub>4</sub> ) in Nm <sup>3</sup> /t (COD)	274	229.2	318.8
Y(CH <sub>4</sub> ) in Nm <sup>3</sup> /t (VS)	421	353.2	489.8

The results of the second batch test with wastewater and inoculum freshly sourced from the AnMBR are shown in Figure A6. The degradation profile of the first and second AnMBR inoculum batch test appears very similar in shape, with a strong increase and a rapid decrease in biogas production after about 4 days. Also, in both batch tests, the biogas production came to a halt after 2 weeks. Only the yields, displayed in Table A6, differ substantially, with a yield of 324 Nm<sup>3</sup>/t (COD) and 498 Nm<sup>3</sup>/t (VS), which is even higher



compared to the standard inoculum. From these results, the conclusion can be drawn that no inhibition of the degradation was found in the AnMBR inoculum batch tests and that the microbial community had adapted to the wastewater substrate to valorise the contained biomolecules more effectively for biogas production compared to the beginning of the continuous feeding experiment.

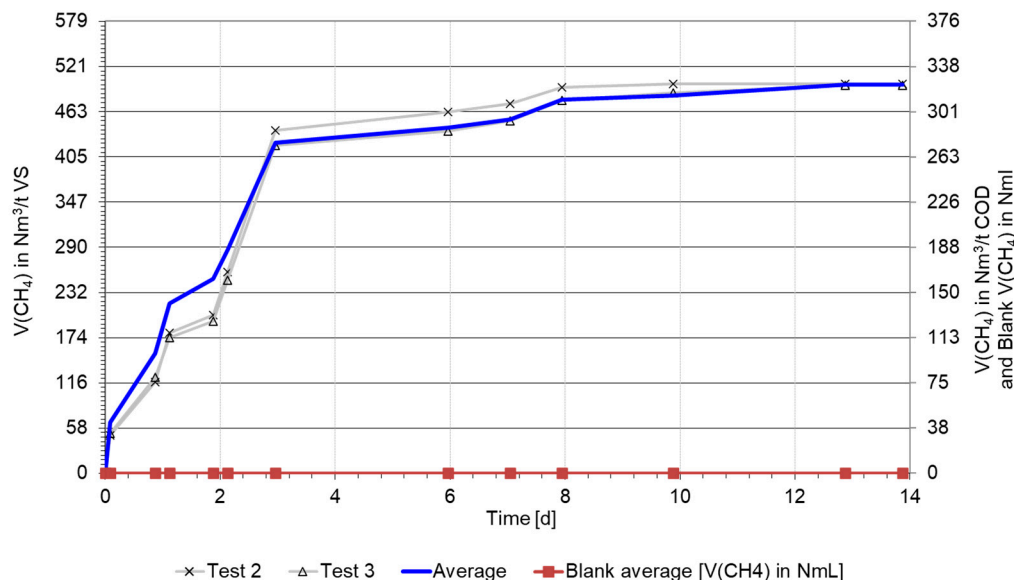


**Figure A6.** Graphical representation of the results of the second batch test with wastewater and the AnMBR inoculum. (SIR = 0.4).

**Table A6.** Table of the batch test results of the second batch test with wastewater and the AnMBR inoculum. (SIR = 0.4).

	Average	Minimum	Maximum
Y(CH <sub>4</sub> ) in Nm <sup>3</sup> /t(FM)	0.6	0.5	0.8
Y(CH <sub>4</sub> ) in Nm <sup>3</sup> /t (COD)	324	270.8	376.6
Y(CH <sub>4</sub> ) in Nm <sup>3</sup> /t (VS)	498	417.2	578.6

To check the validity of the batch tests, a batch test with standard inoculum and a cellulose standard was conducted. The results are shown in Figure A7 and the yields in Table A7. After a short lag phase, the cellulose was sufficiently degraded, and the theoretical yield of 395 Nm<sup>3</sup>/t (VS) was almost reached.

**Table A7.** Table of the batch test results of the control batch test with the cellulose standard and standard inoculum.

	Average	Minimum	Maximum
Y(CH <sub>4</sub> ) in Nm <sup>3</sup> /t(FM)	356.1	299.1	413.2
Y(CH <sub>4</sub> ) in Nm <sup>3</sup> /t (COD)	323.8	271.0	376.9
Y(CH <sub>4</sub> ) in Nm <sup>3</sup> /t (VS)	374.9	314.2	435.8

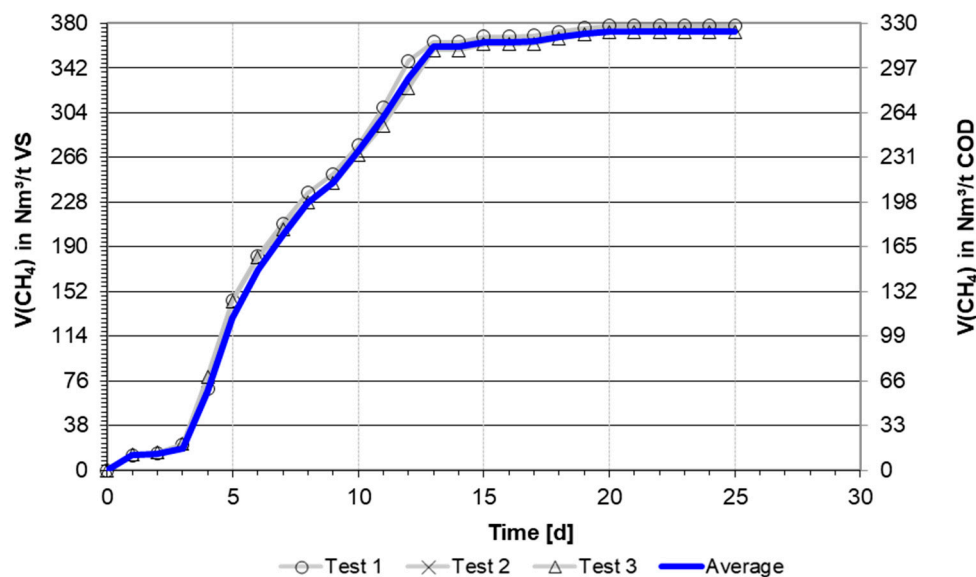


**Figure A7.** Graphical representation of the results of the control batch test with the cellulose standard and standard inoculum.

## References

- Parihar, R.K.; Chaurasia, S.P.; Midda, M.O. An overview of anaerobic membrane bioreactors' evolving research statistics for treating wastewater. *Mater. Today Proc.* **2023**, *102*, 52–58. [\[CrossRef\]](#)
- Lin, H.; Peng, W.; Zhang, M.; Chen, J.; Hong, H.; Zhang, Y. A review on anaerobic membrane bioreactors: Applications, membrane fouling and future perspectives. *Desalination* **2013**, *314*, 169–188. [\[CrossRef\]](#)
- McCarty, P.L.; Bae, J.; Kim, J. Domestic wastewater treatment as a net energy producer—can this be achieved? *Environ. Sci. Technol.* **2011**, *45*, 7100–7106. [\[CrossRef\]](#) [\[PubMed\]](#)
- Inaba, T.; Aoyagi, T.; Hori, T.; Charfi, A.; Suh, C.; Lee, J.H.; Sato, Y.; Ogata, A.; Aizawa, H.; Habe, H. Clarifying prokaryotic and eukaryotic biofilm microbiomes in anaerobic membrane bioreactor by non-destructive microscopy and high-throughput sequencing. *Chemosphere* **2020**, *254*, 126810. [\[CrossRef\]](#)
- Angelidaki, I.; Karakashev, D.; Batstone, D.J.; Plugge, C.M.; Stams, A.J.M. *Methods Enzymol.: Biomethanation and Its Potential*; Elsevier: Amsterdam, The Netherlands, 2011.
- Rodell, M.; Barnoud, A.; Robertson, F.R.; Allan, R.P.; Bellas-Manley, A.; Bosilovich, M.G.; Chambers, D.; Landerer, F.; Loomis, B.; Nerem, R.S.; et al. An Abrupt Decline in Global Terrestrial Water Storage and Its Relationship with Sea Level Change. *Surv. Geophys.* **2024**, *45*, 1875–1902. [\[CrossRef\]](#)
- Souza, C.L.; Chernicharo, C.A.L.; Aquino, S.F. Quantification of dissolved methane in UASB reactors treating domestic wastewater under different operating conditions. *Water Sci. Technol.* **2011**, *64*, 2259–2264. [\[CrossRef\]](#) [\[PubMed\]](#)
- Balcioğlu, G.; Yilmaz, G.; Gönder, Z.B. Evaluation of anaerobic membrane bioreactor (AnMBR) treating confectionery wastewater at long-term operation under different organic loading rates: Performance and membrane fouling. *Chem. Eng. J.* **2021**, *404*, 126261. [\[CrossRef\]](#)
- Chang, S. Anaerobic Membrane Bioreactors (AnMBR) for Wastewater Treatment. *ACES* **2014**, *4*, 56–61. [\[CrossRef\]](#)
- Lin, H.; Gao, W.; Meng, F.; Liao, B.-Q.; Leung, K.-T.; Zhao, L.; Chen, J.; Hong, H. Membrane Bioreactors for Industrial Wastewater Treatment: A Critical Review. *Crit. Rev. Environ. Sci. Technol.* **2012**, *42*, 677–740. [\[CrossRef\]](#)
- Johns, M.R. Developments in Wastewater Treatment in the Meat Processing Industry: A Review. *Bioresour. Technol.* **1995**, *54*, 203–216. [\[CrossRef\]](#)
- Bustillo-Lecompte, C.F.; Mehrvar, M. Slaughterhouse wastewater characteristics, treatment, and management in the meat processing industry: A review on trends and advances. *J. Environ. Manag.* **2015**, *161*, 287–302. [\[CrossRef\]](#) [\[PubMed\]](#)
- Aziz, A.; Basheer, F.; Sengar, A.; Irfanullah; Khan, S.U.; Farooqi, I.H. Biological wastewater treatment (anaerobic-aerobic) technologies for safe discharge of treated slaughterhouse and meat processing wastewater. *Sci. Total Environ.* **2019**, *686*, 681–708. [\[CrossRef\]](#) [\[PubMed\]](#)
- Baker, B.R.; Mohamed, R.; Al-Gheethi, A.; Aziz, H.A. Advanced technologies for poultry slaughterhouse wastewater treatment: A systematic review. *J. Dispers. Sci. Technol.* **2021**, *42*, 880–899. [\[CrossRef\]](#)

15. Yapıcıoğlu, P.; Yeşilnacar, M.İ. Investigating energy costs for a wastewater treatment plant in a meat processing industry regarding water-energy nexus. *Environ. Sci. Pollut. Res.* **2021**, *29*, 1301–1313. [[CrossRef](#)] [[PubMed](#)]
16. Jensen, P.D.; Yap, S.D.; Boyle-Gotla, A.; Janoschka, J.; Carney, C.; Pidou, M.; Batstone, D.J. Anaerobic membrane bioreactors enable high rate treatment of slaughterhouse wastewater. *Biochem. Eng. J.* **2015**, *97*, 132–141. [[CrossRef](#)]
17. Kumar Gautam, R.; Olubukola, A.; More, N.; Jegatheesan, V.; Muthukumaran, S.; Navaratna, D. Evaluation of long-term operational and treatment performance of a high-biomass submerged anaerobic membrane bioreactor treating abattoir wastewater. *Chem. Eng. J.* **2023**, *463*, 142145. [[CrossRef](#)]
18. Tran Thi Viet, N.; Vu, D.C.; Duong, T.H. Effect of Hydraulic retention time on performance of anaerobic membrane bioreactor treating slaughterhouse wastewater. *Environ. Res.* **2023**, *233*, 116522. [[CrossRef](#)]
19. Rouland, G.; Safferman, S.I.; Schwehofer, J.P.; Garmyn, A.J. Characterization of Low-Volume Meat Processing Wastewater and Impact of Facility Factors. *Water* **2024**, *16*, 540. [[CrossRef](#)]
20. Ortner, M.; Leitzinger, K.; Skupien, S.; Bochmann, G.; Fuchs, W. Efficient anaerobic mono-digestion of N-rich slaughterhouse waste: Influence of ammonia, temperature and trace elements. *Bioresour. Technol.* **2014**, *174*, 222–232. [[CrossRef](#)]
21. DIN. *DIN 38 414 Part 4, German Standard Methods for the Examination of Water, Waste Water and Sludge*; DIN: Berlin, Germany, 1984.
22. *DIN 38409-41:1980-12*; Deutsche Einheitsverfahren zur Wasser-, Abwasser- und Schlammuntersuchung; Summarische Wirkungs- und Stoffkenngrößen (Gruppe H); Bestimmung des Chemischen Sauerstoffbedarfs (CSB) im Bereich über 15 mg/L (H 41). DIN Media GmbH: Berlin, Germany, 1980.
23. *DIN EN 16169:2012-11*; Schlamm, behandelte Bioabfall und Boden—Bestimmung des Kjeldahl-Stickstoffs; Deutsche Fassung EN\_16169:2012. DIN Media GmbH: Berlin, Germany.
24. Sriperum, N.; Pesti, G.M.; Tillman, P.B. Evaluation of the fixed nitrogen-to-protein (N:P) conversion factor (6.25) versus ingredient specific N:P conversion factors in feedstuffs. *J. Sci. Food Agric.* **2011**, *91*, 1182–1186. [[CrossRef](#)]
25. *DIN 38414-19:1999-12*; Deutsche Einheitsverfahren zur Wasser-, Abwasser- und Schlammuntersuchung—Schlamm und Sedimente (Gruppe S)—Teil 19: Bestimmung der wasserdampf-flüchtigen organischen Säuren (S 19). DIN Media GmbH: Berlin, Germany, 1999.
26. Rutzmoser, K.; Spann, B. Zielwert-Futteroptimierung. Available online: <https://www.lfl.bayern.de/iba/energie/031560/> (accessed on 30 January 2024).
27. Baserga, U. *Landwirtschaftliche Co-Vergärungs-Biogasanlagen: Biogas aus organischen Reststoffen und Energiegras: FAT-Berichte Nr. 512*; FAT: Bern, Switzerland, 1998.
28. Klindworth, A.; Pruesse, E.; Schweer, T.; Peplies, J.; Quast, C.; Horn, M.; Glöckner, F.O. Evaluation of general 16S ribosomal RNA gene PCR primers for classical and next-generation sequencing-based diversity studies. *Nucleic Acids Res.* **2013**, *41*, e1. [[CrossRef](#)] [[PubMed](#)]
29. National Center for Biotechnology Information. BioProject PRJNA1198955. Available online: <https://www.ncbi.nlm.nih.gov/sra/PRJNA1198955> (accessed on 30 January 2024).
30. Babraham Bioinformatics. FastQC: A Quality Control Tool for High Throughput Sequence Data. Available online: <http://www.bioinformatics.babraham.ac.uk/projects/fastqc/> (accessed on 30 January 2024).
31. Martin, M. Cutadapt removes adapter sequences from high-throughput sequencing reads. *EMBnet J.* **2011**, *17*, 10. [[CrossRef](#)]
32. Edgar, R.C. Search and clustering orders of magnitude faster than BLAST. *Bioinformatics* **2010**, *26*, 2460–2461. [[CrossRef](#)] [[PubMed](#)]
33. Edgar, R.C. UNOISE2: Improved error-correction for Illumina 16S and ITS amplicon sequencing. *BioRxiv* **2016**. [[CrossRef](#)]
34. Edgar, R.C. UNCROSS2: Identification of Cross-Talk in 16S rRNA OTU Tables. *BioRxiv* **2018**. [[CrossRef](#)]
35. Edgar, R.C. SINTAX: A Simple non-Bayesian Taxonomy Classifier for 16S and ITS Sequences. *BioRxiv* **2016**. [[CrossRef](#)]
36. Oksanen, J.; Simpson, G.; Blanchet, F.; Kindt, R.; Legendre, P.; Minchin, P.; O'Hara, R.; Solymos, P.; Stevens, M.; Szoecs, E.; et al. Vegan (Community Ecology Package). Available online: <https://CRAN.R-project.org/package=vegan> (accessed on 30 January 2024).
37. R Core Team. R: A Language and Environment for Statistical Computing. Available online: <https://www.R-project.org> (accessed on 30 January 2024).
38. Latiffi, N.A.A.; Mohamed, R.M.S.R.; Al-Gheethi, A.; Tajuddin, R.M.; Al-Shaibani, M.M.; Vo, D.-V.N.; Rupani, P.F. Nutrients elimination from meat processing wastewater using *Scenedesmus* sp.; optimizations; artificial neural network and kinetics models. *Environ. Technol. Innov.* **2022**, *26*, 102535. [[CrossRef](#)]
39. Galib, M.; Elbeshbishy, E.; Reid, R.; Hussain, A.; Lee, H.-S. Energy-positive food wastewater treatment using an anaerobic membrane bioreactor (AnMBR). *J. Environ. Manag.* **2016**, *182*, 477–485. [[CrossRef](#)]
40. Handous, N. Two-Stage Anaerobic Digestion of Meat Processing Solid Wastes: Methane Potential Improvement with Wastewater Addition and Solid Substrate Fermentation. *Waste Biomass Valor.* **2019**, *10*, 131–142. [[CrossRef](#)]

41. Atlas Scientific. The Importance Of Electrical Conductivity of Wastewater. Available online: <https://atlas-scientific.com/blog/electrical-conductivity-of-wastewater/> (accessed on 20 December 2024).
42. Malmberg, C.G. Electrical Conductivity of Dilute Solutions of "Sea Water" From 5 to 120 °C. *J. Res. Natl. Bur. Stand. A Phys. Chem.* **1965**, *69A*, 39–43. [[CrossRef](#)]
43. Vinogradova, O.I.; Silkina, E.F. Conductivity of concentrated salt solutions. *arXiv* **2023**, arXiv:2312.02624. [[CrossRef](#)]
44. Painter, T. How To Convert Conductivity To Concentration. Available online: <https://www.sciencing.com/convert-conductivity-concentration-6925703/> (accessed on 20 December 2024).
45. Ali, N.S.; Mo, K.; Kim, M. A case study on the relationship between conductivity and dissolved solids to evaluate the potential for reuse of reclaimed industrial wastewater. *KSCE J. Civ. Eng.* **2012**, *16*, 708–713. [[CrossRef](#)]
46. Klein, R.; Slaný, V.; Krčálová, E. Conductivity Measurement for Control of a Biogas Plant. *Acta Univ. Agric. Silvic. Mendel. Brun.* **2018**, *66*, 1151–1156. [[CrossRef](#)]
47. Rosenberg, E.; DeLong, E.F.; Lory, S.; Stackebrandt, E.; Thompson, F. *The Prokaryotes*; Springer: Berlin/Heidelberg, Germany, 2013; ISBN 978-3-642-30140-7.
48. Silver, S.; Walderhaug, M. Gene regulation of plasmid- and chromosome-determined inorganic ion transport in bacteria. *Microbiol. Rev.* **1992**, *56*, 195–228. [[CrossRef](#)] [[PubMed](#)]
49. Gao, Q.; Zhang, Y.; Li, L.; Zhou, H.; Wang, K.; Ding, J.; Jiang, J.; Wei, L.; Zhao, Q. The stress of bioactive compounds on microbes in anaerobic digestion of food waste and mitigation strategies: A critical review. *Chem. Eng. J.* **2024**, *493*, 152746. [[CrossRef](#)]
50. Li, Y.; Zhang, S.; Chen, Z.; Ye, Z.; Lyu, R. Multi-omics analysis unravels effects of salt and oil on substance transformation, microbial community, and transcriptional activity in food waste anaerobic digestion. *Bioresour. Technol.* **2023**, *387*, 129684. [[CrossRef](#)] [[PubMed](#)]
51. Basset, N.; Santos, E.; Dosta, J.; Mata-Álvarez, J. Start-up and operation of an AnMBR for winery wastewater treatment. *Ecol. Eng.* **2016**, *86*, 279–289. [[CrossRef](#)]
52. Fuchs, W.; Binder, H.; Mavrias, G.; Braun, R. Anaerobic treatment of wastewater with high organic content using a stirred tank reactor coupled with a membrane filtration unit. *Water Res.* **2003**, *37*, 902–908. [[CrossRef](#)]
53. Heidrich, E.S.; Curtis, T.P.; Dolfin, J. Determination of the internal chemical energy of wastewater. *Environ. Sci. Technol.* **2011**, *45*, 827–832. [[CrossRef](#)]
54. Wahaab, R.A.; El-awady, M.H. Anaerobic/aerobic treatment of meat processing wastewater. *Environmentalist* **1999**, *19*, 61–65. [[CrossRef](#)]
55. Bundeskanzleramt der Republik Österreich. BGBl. II Nr. 12/1999 Verordnung des Bundesministers für Land- und Forstwirtschaft über die Begrenzung von Abwasseremissionen aus der Schlachtung und Fleischverarbeitung: AEV Fleischwirtschaft. Available online: <https://www.ris.bka.gv.at/GeltendeFassung.wxe?Abfrage=Bundesnormen&Gesetzesnummer=1001150&FassungVom=2019-06-24> (accessed on 20 December 2024).
56. Li, W.-W.; Yu, H.-Q.; Rittmann, B.E. Chemistry: Reuse water pollutants. *Nature* **2015**, *528*, 29–31. [[CrossRef](#)]
57. Ortner, M.; Wöss, D.; Schumergruber, A.; Pröll, T.; Fuchs, W. Energy self-supply of large abattoir by sustainable waste utilization based on anaerobic mono-digestion. *Appl. Energy* **2015**, *143*, 460–471. [[CrossRef](#)]
58. Smith, A.L.; Stadler, L.B.; Cao, L.; Love, N.G.; Raskin, L.; Skerlos, S.J. Navigating wastewater energy recovery strategies: A life cycle comparison of anaerobic membrane bioreactor and conventional treatment systems with anaerobic digestion. *Environ. Sci. Technol.* **2014**, *48*, 5972–5981. [[CrossRef](#)]
59. Pan, S.-Y.; Snyder, S.W.; Packman, A.I.; Lin, Y.J.; Chiang, P.-C. Cooling water use in thermoelectric power generation and its associated challenges for addressing water-energy nexus. *Water-Energy Nexus* **2018**, *1*, 26–41. [[CrossRef](#)]
60. Liu, Z.; Yin, H.; Dang, Z.; Liu, Y. Dissolved methane: A hurdle for anaerobic treatment of municipal wastewater. *Environ. Sci. Technol.* **2014**, *48*, 889–890. [[CrossRef](#)] [[PubMed](#)]
61. U.S. EPA, OAR, Climate Change Division. *Global Anthropogenic Non-CO2 Greenhouse Gas Emissions: 1990–2030: EPA 430-R-12-006*; U.S. EPA, OAR, Climate Change Division: Washington, DC, USA, 2012.
62. Sander, R. Compilation of Henry's law constants (version 4.0) for water as solvent. *Atmos. Chem. Phys.* **2015**, *15*, 4399–4981. [[CrossRef](#)]
63. Velasco, P.; Jegatheesan, V.; Othman, M. Recovery of Dissolved Methane From Anaerobic Membrane Bioreactor Using Degassing Membrane Contactors. *Front. Environ. Sci.* **2018**, *6*, 151. [[CrossRef](#)]
64. Yeo, H.; An, J.; Reid, R.; Rittmann, B.E.; Lee, H.-S. Contribution of Liquid/Gas Mass-Transfer Limitations to Dissolved Methane Oversaturation in Anaerobic Treatment of Dilute Wastewater. *Environ. Sci. Technol.* **2015**, *49*, 10366–10372. [[CrossRef](#)] [[PubMed](#)]
65. Smith, A.L.; Skerlos, S.J.; Raskin, L. Psychrophilic anaerobic membrane bioreactor treatment of domestic wastewater. *Water Res.* **2013**, *47*, 1655–1665. [[CrossRef](#)] [[PubMed](#)]

66. Thakur, N.; Jalalah, M.; Alsareii, S.A.; Harraz, F.A.; Almadiy, A.A.; Su, S.; Salama, E.-S.; Li, X. Anaerobic digestion of fat, oil, and grease (FOG) under combined additives: Enhanced digestibility, biogas production, and microbiome. *Renew. Sustain. Energy Rev.* **2024**, *191*, 114155. [[CrossRef](#)]
67. Guo, Z.; Usman, M.; Alsareii, S.A.; Harraz, F.A.; Al-Assiri, M.S.; Jalalah, M.; Li, X.; Salama, E.-S. Synergistic ammonia and fatty acids inhibition of microbial communities during slaughterhouse waste digestion for biogas production. *Bioresour. Technol.* **2021**, *337*, 125383. [[CrossRef](#)] [[PubMed](#)]

**Disclaimer/Publisher's Note:** The statements, opinions and data contained in all publications are solely those of the individual author(s) and contributor(s) and not of MDPI and/or the editor(s). MDPI and/or the editor(s) disclaim responsibility for any injury to people or property resulting from any ideas, methods, instructions or products referred to in the content.